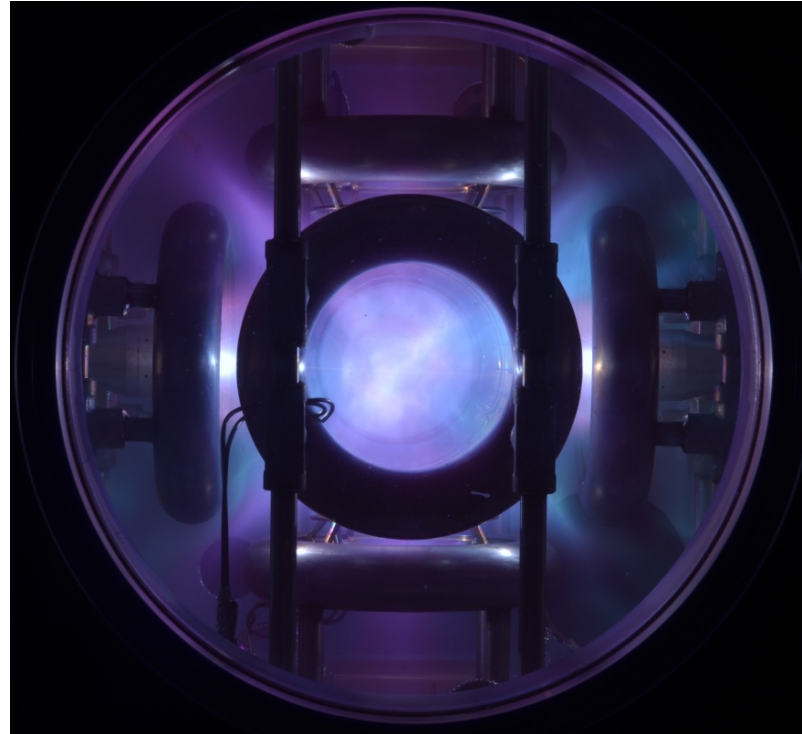


Polywell – A Path to Electrostatic Fusion



Jaeyoung Park
Energy Matter Conversion Corporation (EMC2)
University of Wisconsin, October 1, 2014

Fusion vs. Solar Power

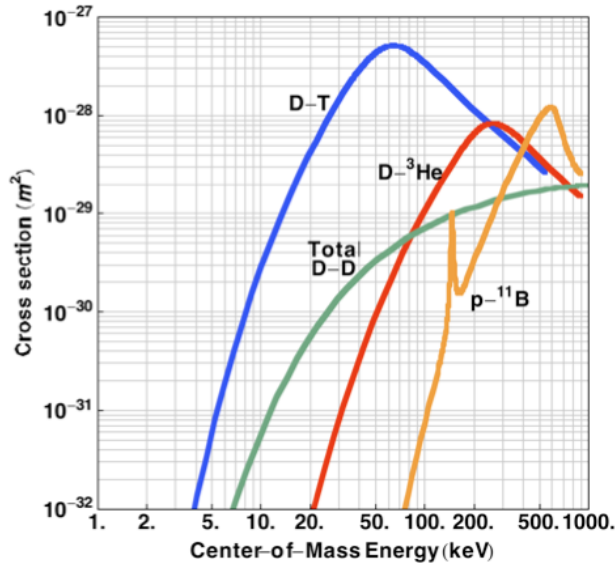


Figure 1. Fusion cross sections versus center-of-mass energy



200 W/m²: available solar panel capacity

For a 50 cm radius spherical IEC device

- Area projection: $\pi r^2 = 7850 \text{ cm}^2$

→ 160 watt for same size solar panel

$$P_{fusion} = 17.6 \text{ MeV} \times \int \langle \sigma v \rangle \times (n_D n_T) dV$$

For D-T: 160 Watt → $5.7 \times 10^{13} \text{ n/s}$

$\langle \sigma v \rangle_{max} \sim 8 \times 10^{-16} \text{ cm}^3/\text{s}$

→ $\langle n_e \rangle \sim \underline{7 \times 10^{11} \text{ cm}^{-3}}$

Debye length $\sim 0.22 \text{ cm}$ (at 60 keV)

Radius/ $\lambda_D \sim 220$

In comparison, 60 kV well over 50 cm

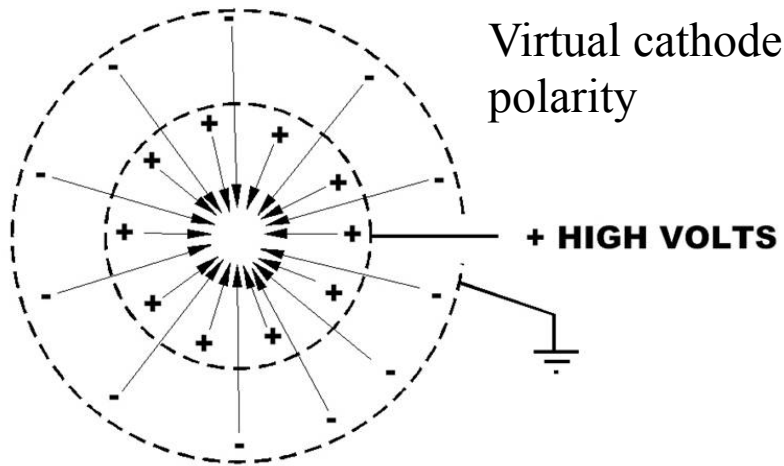
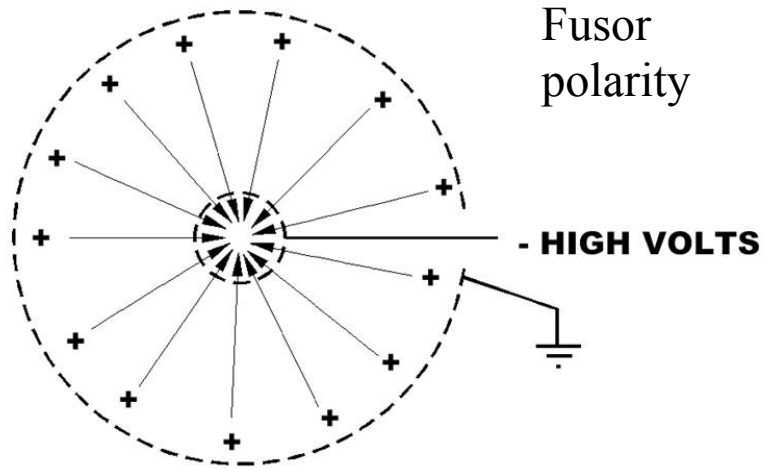
$(n_e - n_i) \sim \underline{4 \times 10^7 \text{ cm}^{-3}}$

0D Analysis - No ion convergence case

Outline

- Polywell Fusion:
 - Electrostatic Fusion + Magnetic Confinement
- Lessons from WB-8 experiments
- Recent Confinement Experiments at EMC2
- Future Work and Summary

Electrostatic Fusion



Contributions from Farnsworth, Hirsch, Elmore, Tuck, Watson and others

Operating principles

(virtual cathode type)

- e-beam (and/or grid) accelerates electrons into center
- Injected electrons form a potential well
- Potential well accelerates/confines ions
- Energetic ions generate fusion near the center

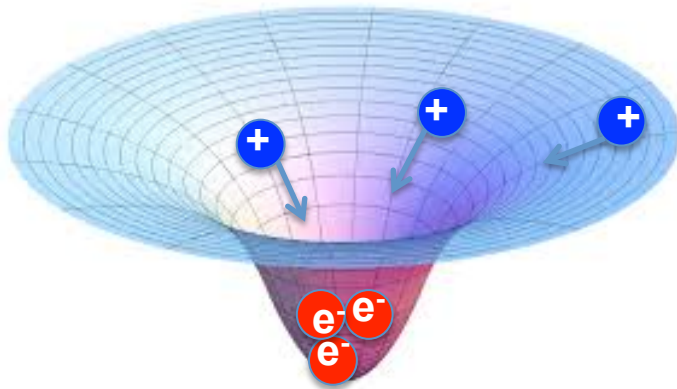
Attributes

- **No ion grid loss**
- **Good ion confinement & ion acceleration**
- **But loss of high energy electrons is too large**

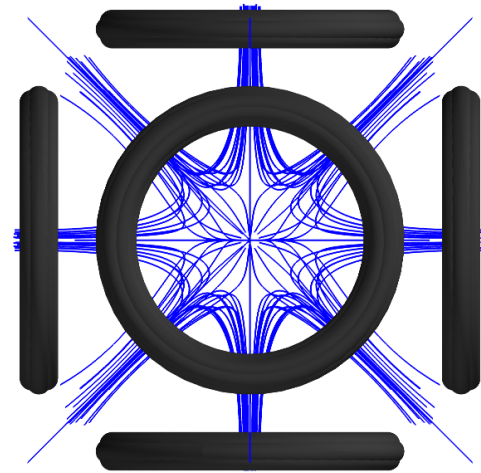
Polywell Fusion

Combines two good ideas in fusion research: Bussard (1985)

- a) **Electrostatic fusion:** High energy electron beams form a potential well, which accelerates and confines ions
- b) **High β magnetic cusp:** High energy electron confinement in high β cusp: Bussard termed this as “wiffle-ball” (WB).



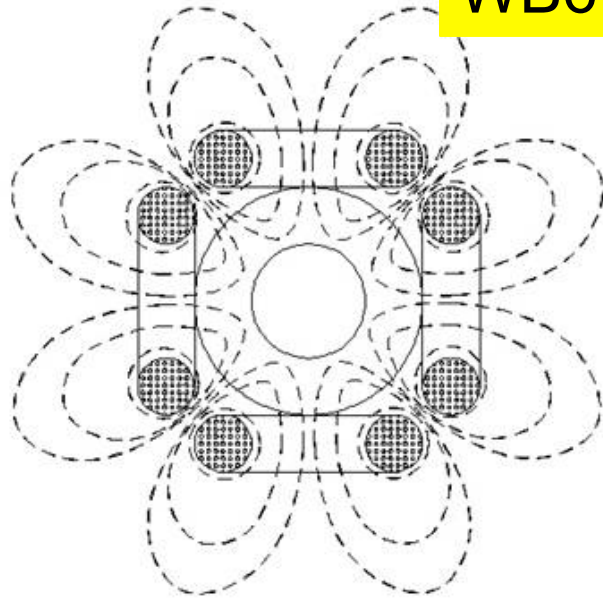
Potential Well: ion heating & confinement



Polyhedral coil cusp: electron confinement

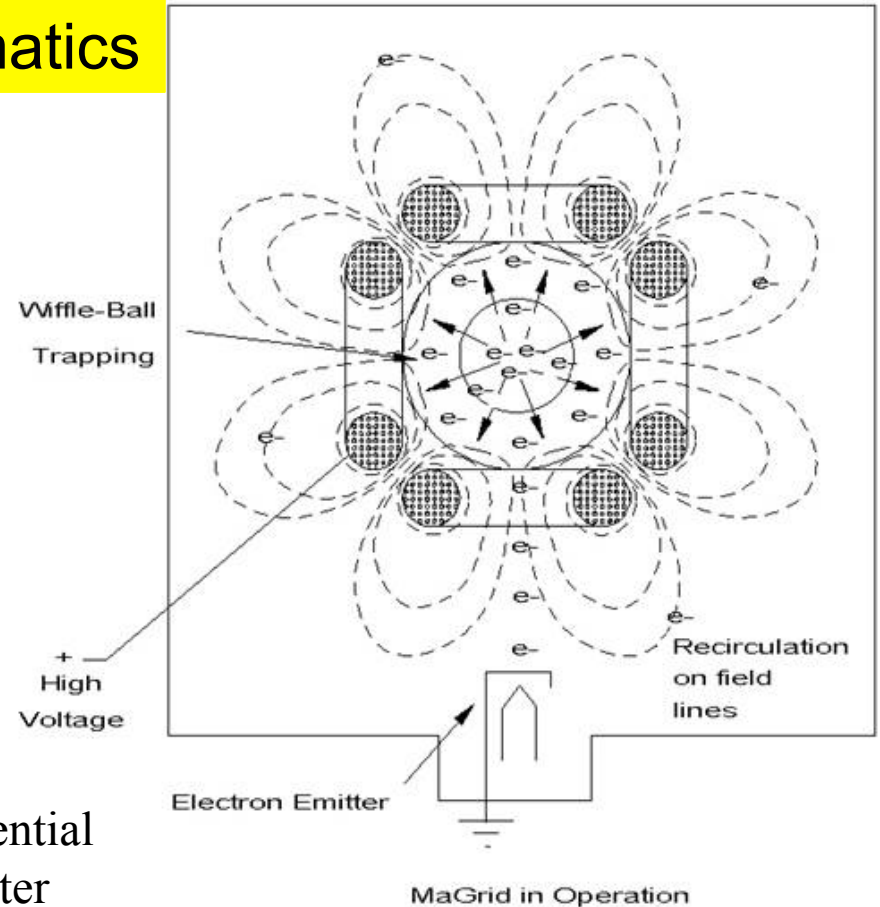
Wiffle-Ball (WB) vs. Magnetic Grid (MaGrid)

WB6 Schematics



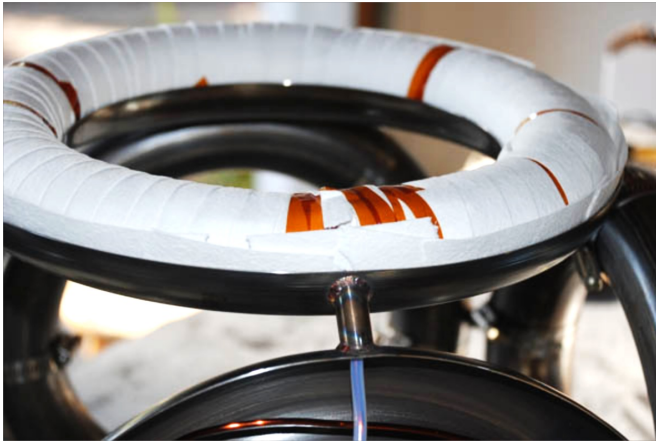
Basic MaGrid Field

- Coil shells are biased to + HV
- Electron injectors & chamber at ground potential
- +HV on coil accelerates electrons to the center
- WB will form once the core plasma reaches sufficient pressure (with power from coil shell)
- Electron recirculation improves confinement

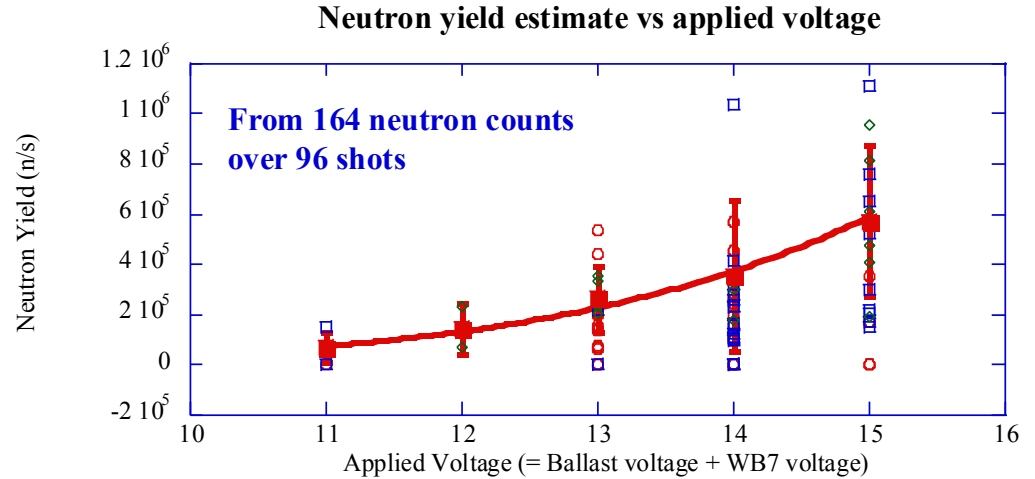


MaGrid in Operation

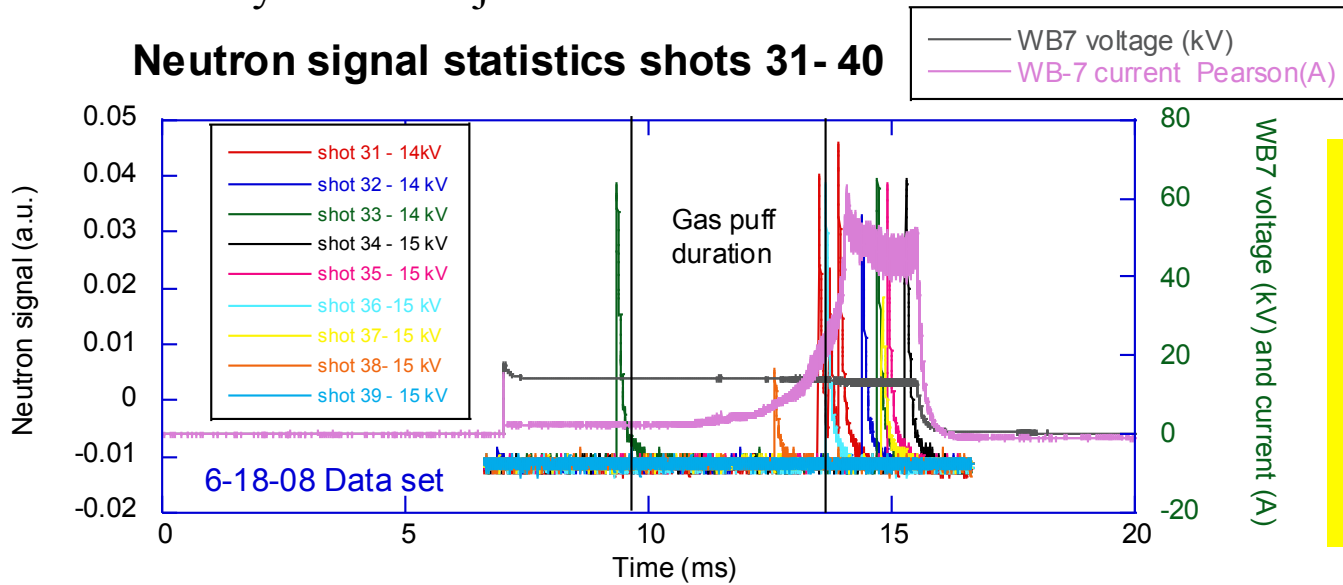
Wiffle-Ball 7 Results



6 coil system with joints

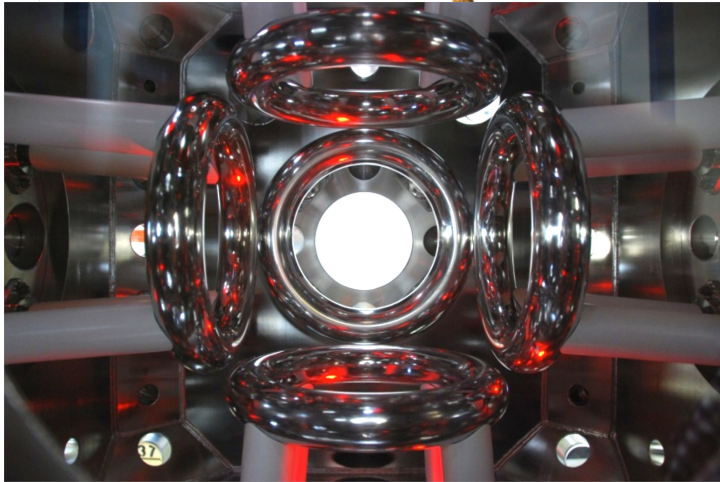
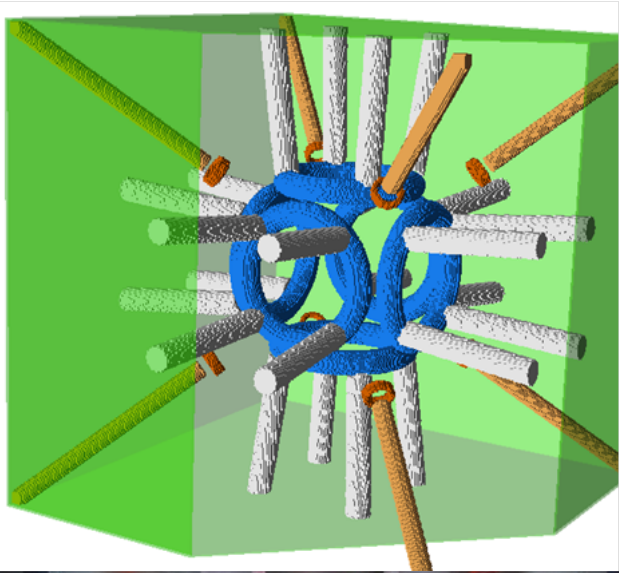


Neutron signal statistics shots 31- 40



- Synchronous detection of neutrons
- Reasonable neutron yields despite low bias voltages
- Confirms WB-6 results

Wiffle-Ball 8 Experiments



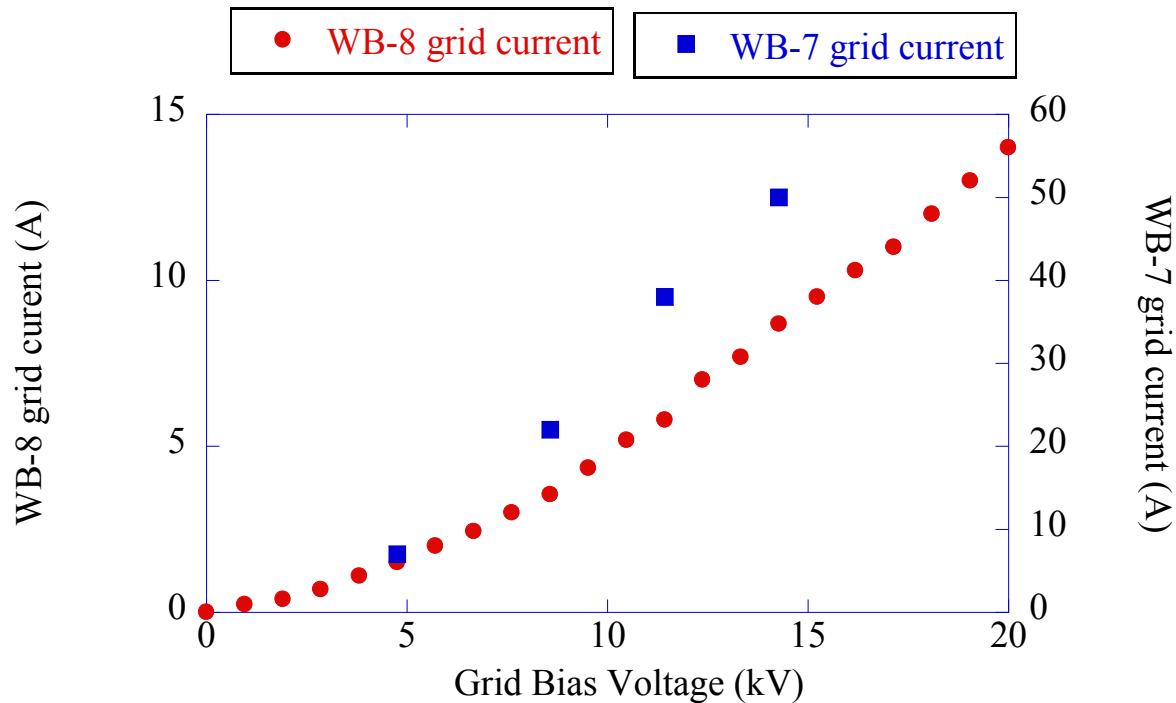
Two major improvements over WB-7

- WB-8 has externally held coils without joints
- WB-8 has an arc plasma source to initiate high density plasmas in the core

Powerful plasma heating to achieve high beta plasmas and wiffleball

- Grid bias: up to 2 kA @50 kV
(500A @ 15kV for WB-7)
- Arc source: 500A arc source for plasma start-up
(None for WB-7)
- 8 Electron injectors: 10A per gun
(~1-2A/gun for WB-7)
- Ion injection: 1 MW (40A at 25 kV) via NBI
(None for WB-7)

Comparison of WB-7 and WB-8



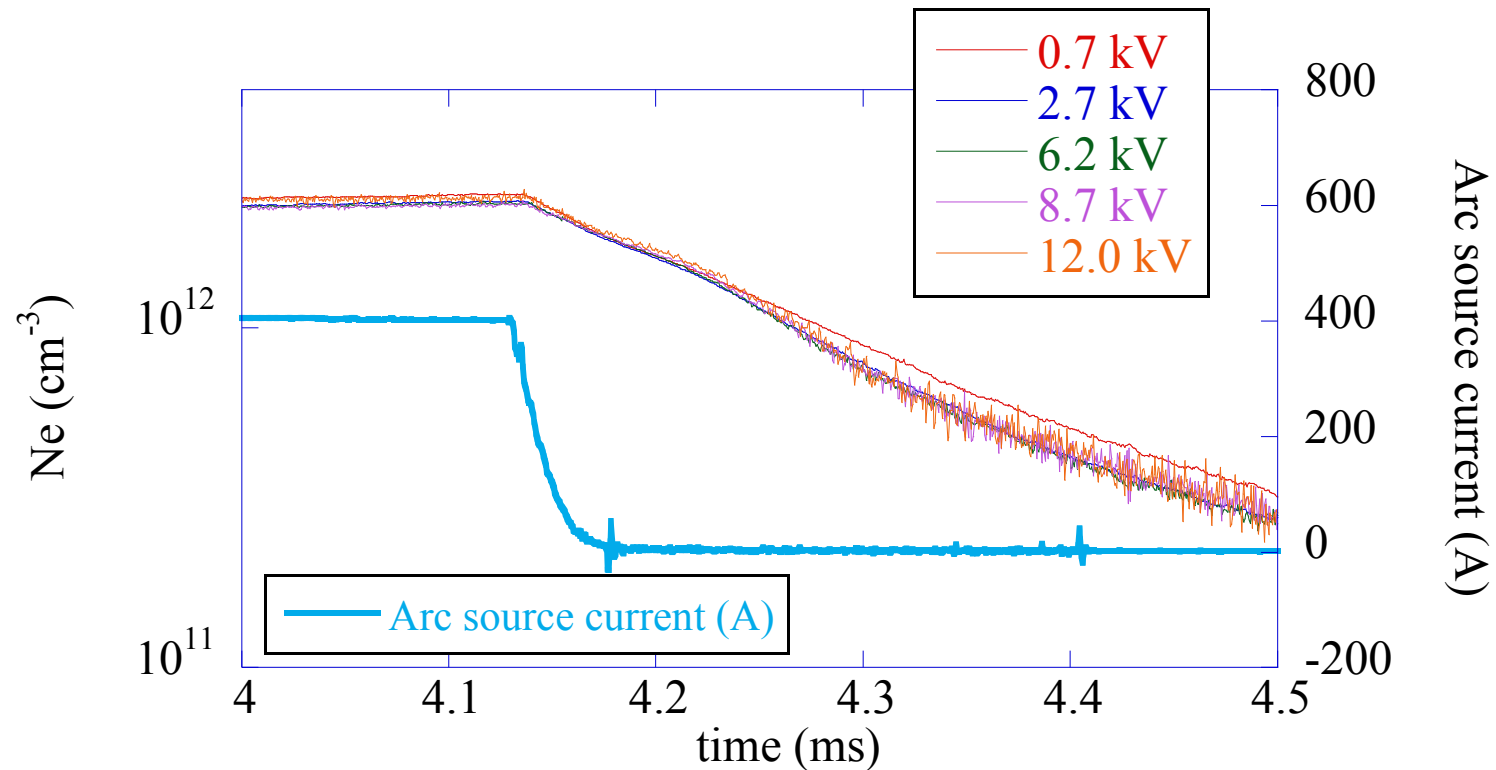
For the same grid bias: WB-8 operate with lower grid current than WB-7, while WB-8 has 6x higher plasma density (WB-8: $3 \times 10^{12} \text{ cm}^{-3}$ and WB-7: $5 \times 10^{11} \text{ cm}^{-3}$)

→ No coil joints

→ Operates with higher B-fields (2 kG for WB-8 and 1 kG for WB-7)

Plasma density decay vs. grid bias

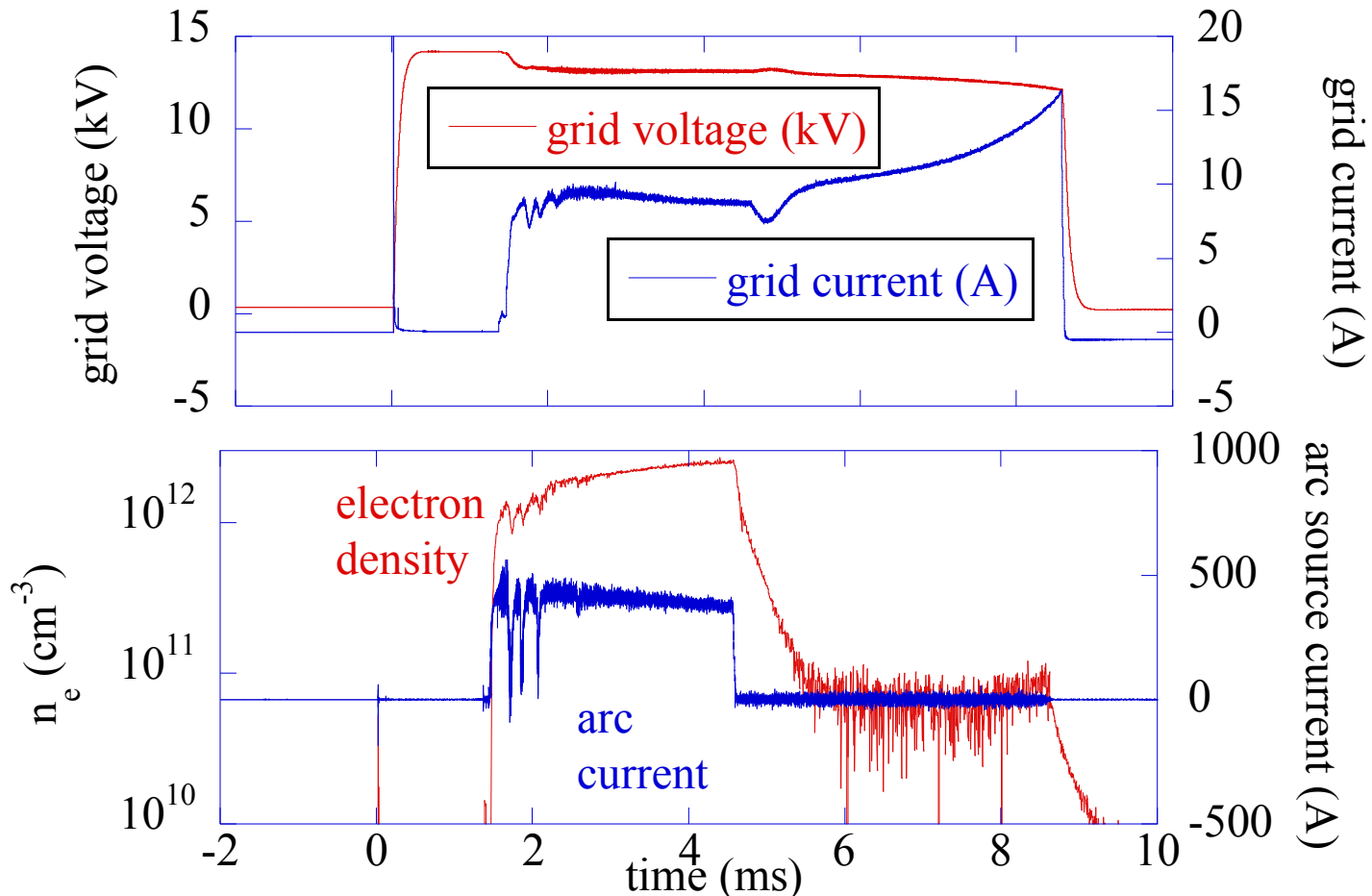
B-field at 2.0 kG, Arc source on for 3 ms, no electron injection and no NBI



No change in n_e decay time ($\sim 180 \mu\text{s}$) vs. grid bias voltage

HV bias on the grid alone cannot sustain plasma density

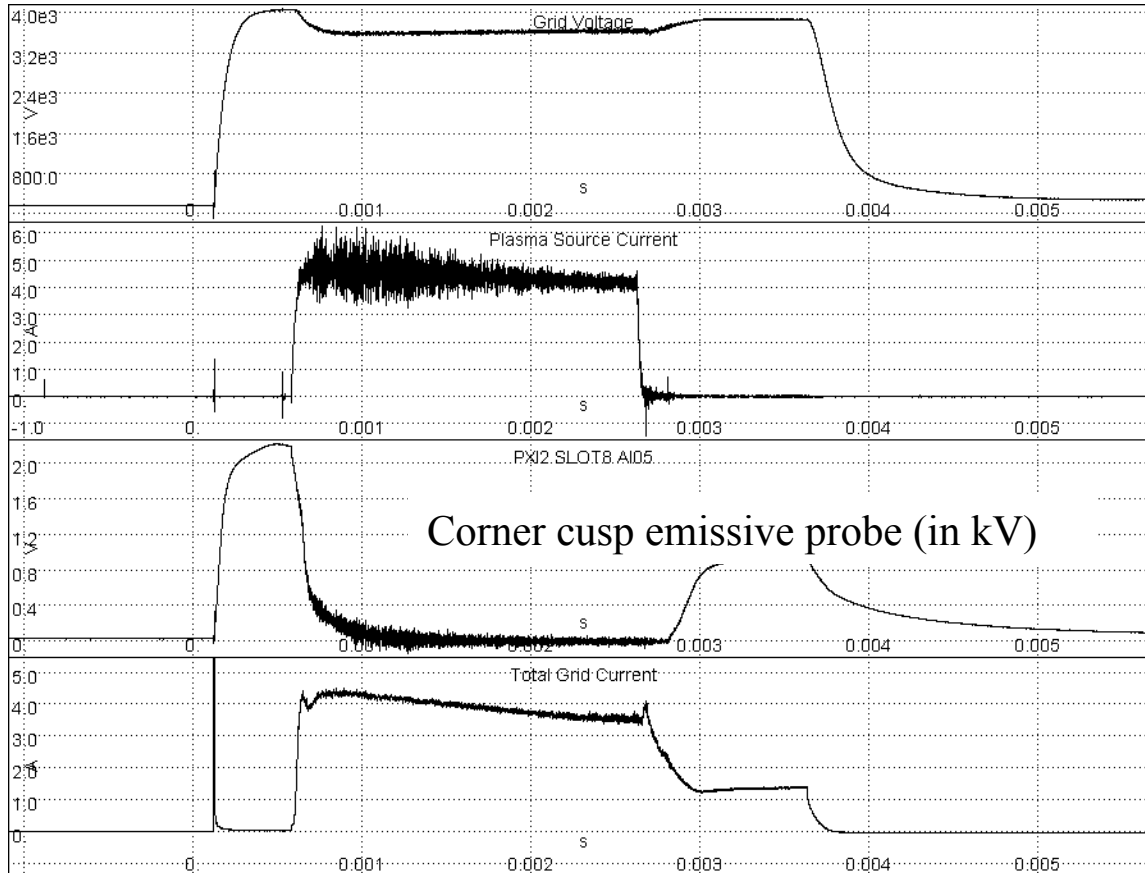
Shot 10625: B-field at 2 kG, 13.2 kV bias, HV with arc source



HV bias and no other source terms \rightarrow Low electron density

Plasma potential measurement

Shot 11010: 2kG, 4 kV bias and arc source (no e-guns)



Plasma potential at the corner cusp drops to 0V with increasing plasma density
→ Grid biasing does not look promising for Potential Well formation

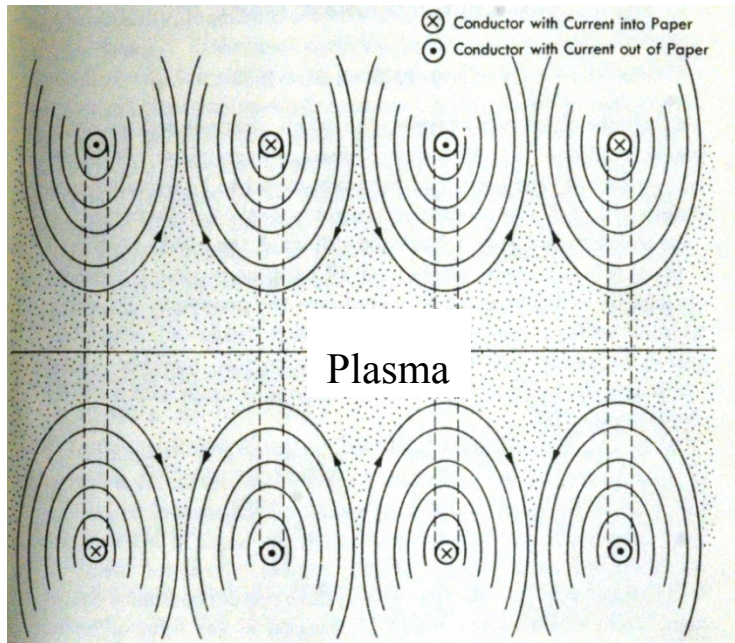
Motivation for Cusp Confinement

Reference: “Project Sherwood: The U. S. Program in Controlled Fusion” by Bishop (1958).

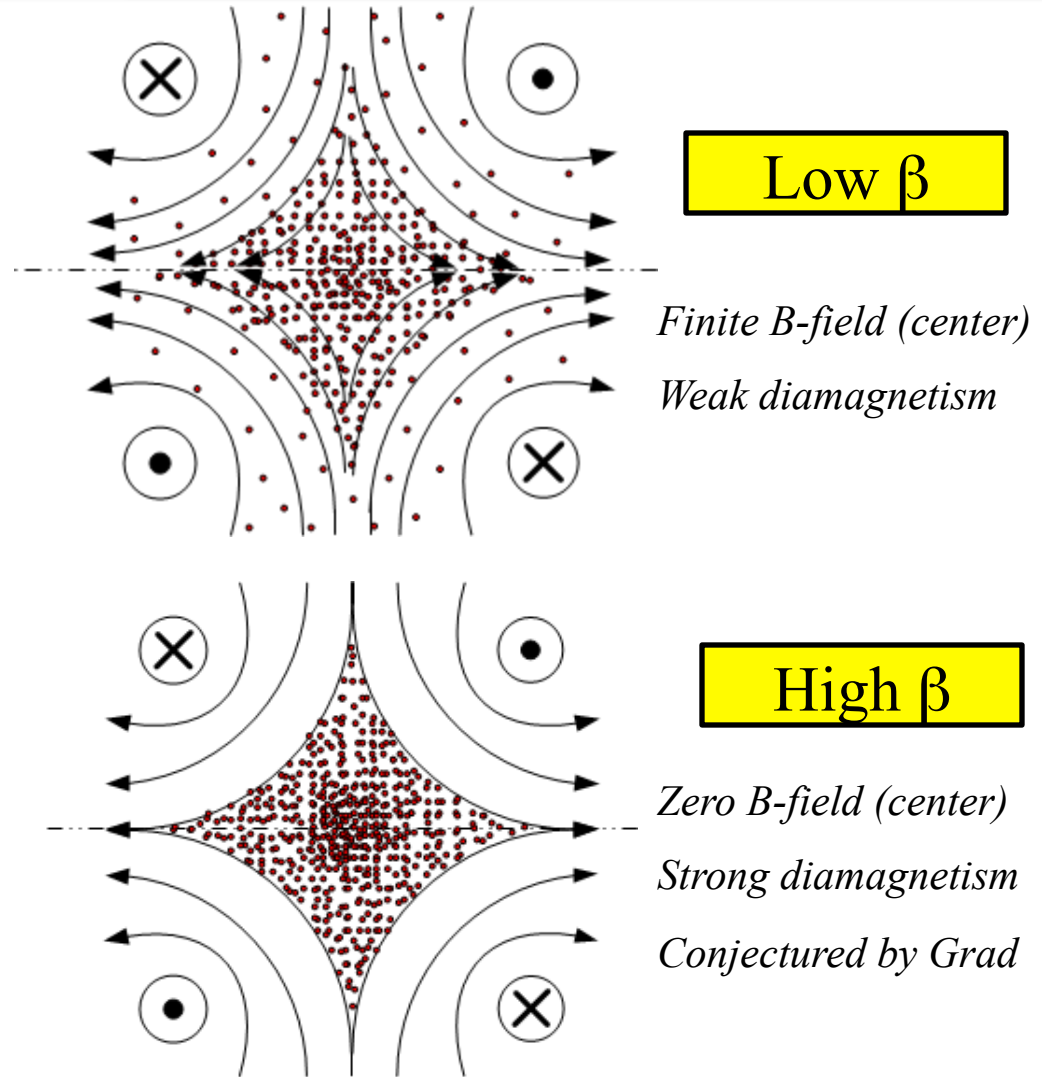
- Question on Plasma Stability by Teller in 1954
 - “Attempts to contain a plasma as somewhat similar to contain jello using rubber bands”
 - Basis of interchange instability (plasma version of Rayleigh Taylor instability) and idea of “good curvature” vs. “bad curvature”
- Preliminary analysis (by Frieman in 1955) indicated stellarator and magnetic mirror would be unstable not just at high β but at all values of β . ($\beta = \text{plasma pressure/magnetic pressure}$)
- By 1957, several concepts such as magnetic shear, field line tying and rotating plasmas were introduced to stabilize stellarator and mirror. However, it is understood that there would be undesirable limits on maximum plasma β in many of magnetic fusion concepts.
- ITER design calls for β to be 0.03, while the fusion power output scales as β^2 for a fixed magnetic field value. H. York at Livermore was concerned that “the limitation on β might so reduce the net power output that this device (stellarator) could never be of economic interest” and started magnetic mirror program at Livermore.

Cusp Confinement Configuration

Picket Fence



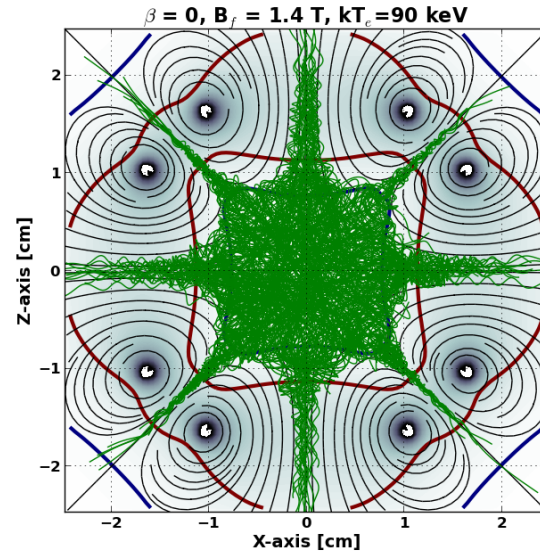
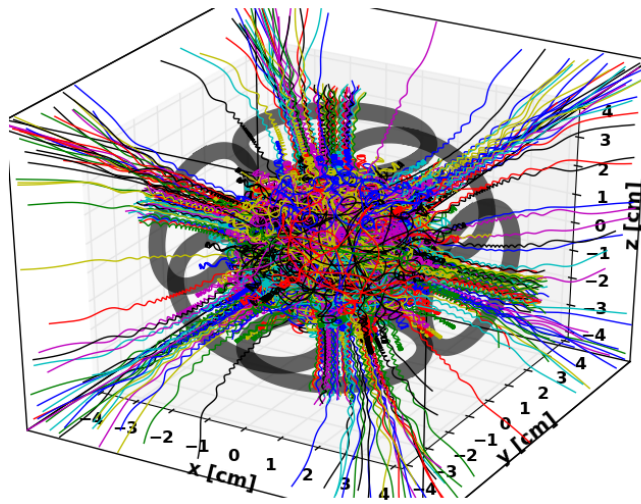
*Conceived by Tuck in 1954
(from Bishop's book)*



Brief History of Cusp Confinement

- Picket-Fence (cusp confinement) concept by Tuck is the first stable magnetic confinement scheme against interchange instability. The entire region of confined plasma faces magnetic fields with good curvature. As such, good plasma stability has been observed in many cusp experiments.
- However, original picket fence approach was quickly abandoned due to rapid plasma loss along the open field lines, meaning good stability comes with bad confinement.
- Between 1955-1958, NYU group led by Grad investigated the case of high β confinement in magnetic cusp. **Their result was the plasma confinement would be greatly enhanced for a high β plasma in the cusp, compared to a low β plasma.**
- This confinement enhancement conjecture made the cusp approach to be promising. For the next 20 years, detailed experiments were conducted on ~ 20 different devices and ~ 200 papers were published related to the cusp confinement as a result. Two excellent review articles by Spalding (1971) and Haines (1977).
- However, most efforts on cusp confinement stopped by 1980 due to a lack of progress.

Plasma Confinement in Cusp at Low β



Low β cusp confinement can be modeled as “magnetic mirror” with particle transit time as a scattering time to loss cone: due to non-conserved magnetic moment near $r=0$

$$\tau_e(r_{coil}, E_e, B_{max}) \approx (2r_{coil} / v_e) \times M^* \text{ or } \propto (r_{coil})^{1.75} \times E_e^{-7/8} \times B_{max}^{3/4}$$

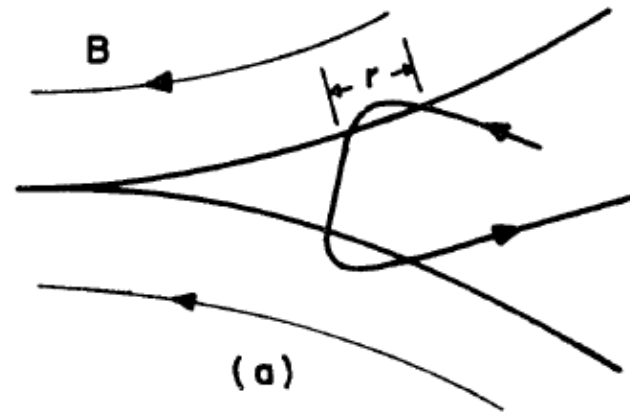
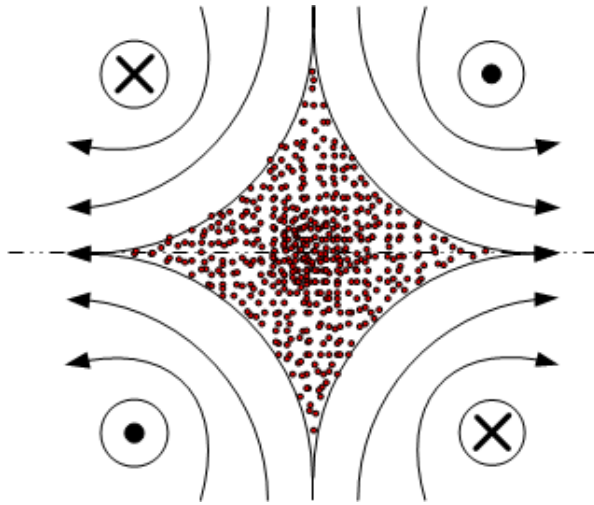
where v_e is a electron velocity at E_e , M^* is an effective mirror ratio, B_{max}/B_{min}^*

$$\text{and } B_{min}^* \text{ is given as } \frac{1}{B} \times \frac{dB}{dr} (r = r_{adibatic}) = \frac{1}{A \times r_{Lamor} (E_e, B_{min}^* (r = r_{adibatic}))}$$

and A is a constant between 3-5 for a given magnetic field profile

1 μ s confinement time
for 100 keV electron with 7
T, 1 m, 6 coil cusp – will not
work for a net power device

Plasma Confinement in Cusp at High β



Berkowitz et al
1958 paper
“Cusped geometries”

In high β cusp, **a sharp transition layer exists between plasma and B-fields**. Plasma particles will undergo specular reflection at the boundary except for the particle moving almost exactly in the direction of the cusp. The loss rate will have gyro-radius scaling.

Theoretically conjectured

Loss current per cusp by Grad and NYU team

$$\frac{I_{e,i}}{e} = \frac{\pi}{9} n_{e,i} v_{e,i} \times \pi (r_{e,i}^{gyro})^2$$



0.5s confinement time
for 100 keV electron with 7 T, 1m,
6 coil cusp → favorable for a net
power device.

What were the challenges on High β cusp?

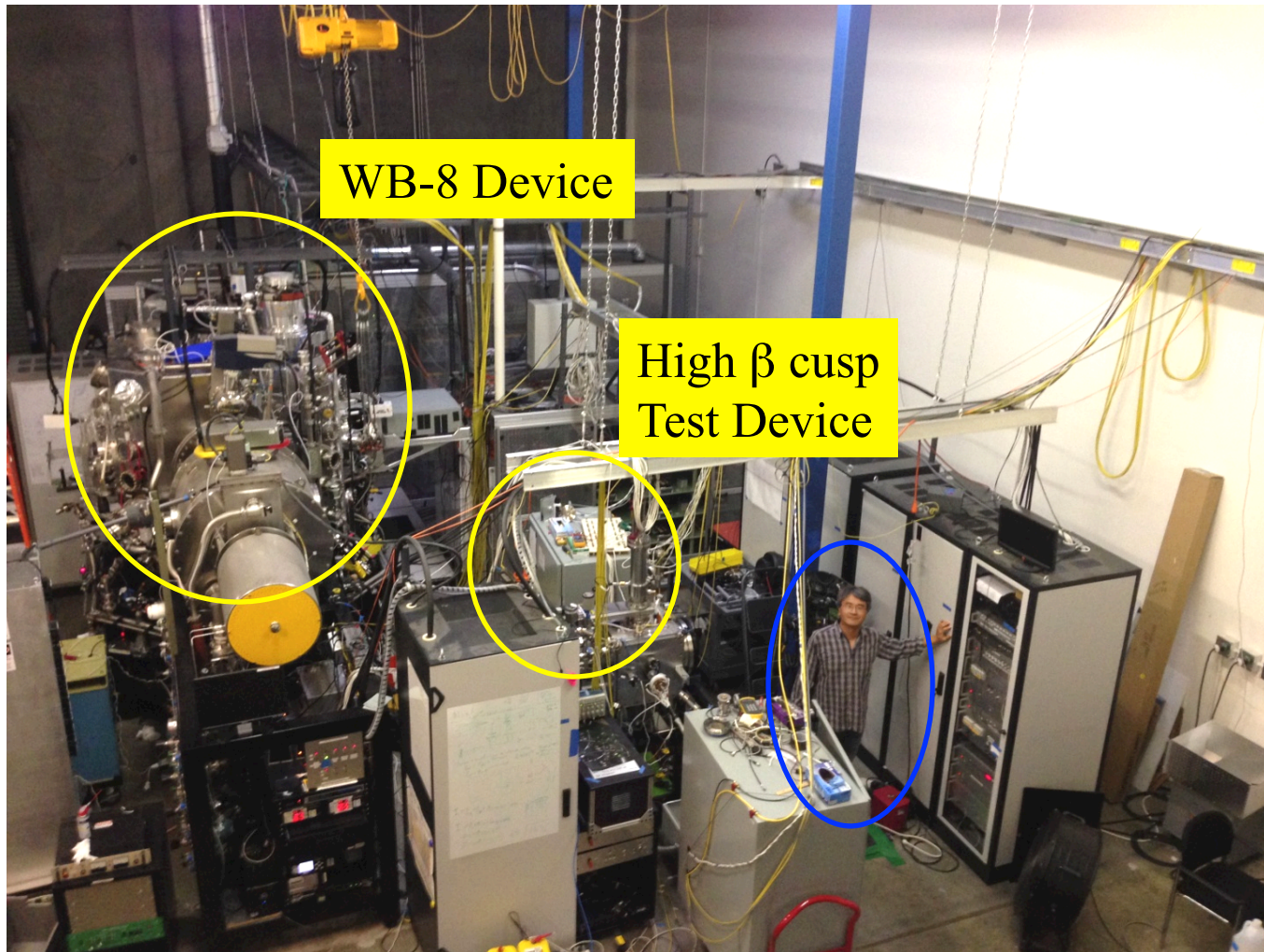
1. **How to form high β plasma in a leaky cusp: start up problem**
 - Use of (pulsed) high power plasma injectors or laser ablation
 - Typical injector produce cold plasmas 10-50 eV
 - $\beta=1$ plasma were achieved with strong diamagnetism and good stability
2. **Which loss rate is correct?**
 - Question on ion gyro-radius vs. electron gyro-radius
 - Ion gyro-radius will not work for fusion: experiments indicated ion gyro-radius
3. **How to heat initial cold plasmas to fusion relevant temperatures?**
 - Magnetic compression and shock heating was suggested and tried without much success.
4. **How to measure plasma confinement or confinement enhancement?**
 - Experiments lasted only for a short period (due to high power injector), while the predicted confinement time was long.

Success on #1, but results on #2 appeared not favorable

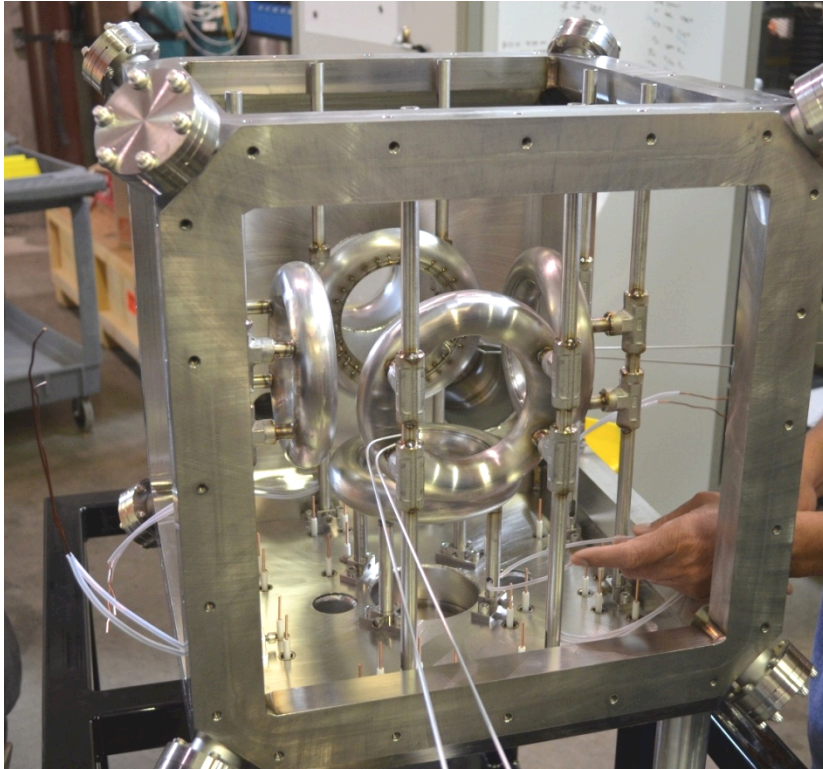
No promising solutions were presented for #3 and #4. → end of cusp by 1980

Recent Experiments at EMC2

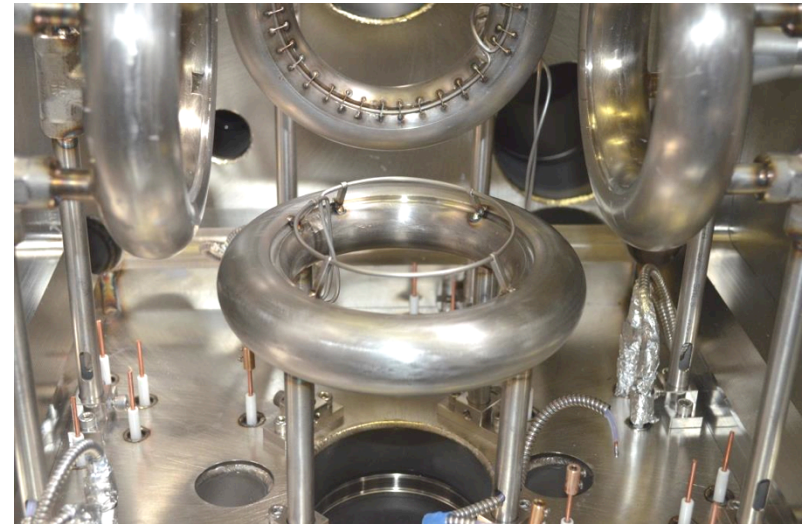
(EMC2 San Diego Facility)



High β cusp test device installation



6 coil cusp installation



Locations of flux loop

Experimental Plan

1. Plasma injection to the cusp

- Use high power arc (solid target) plasma injectors

2. Verify high β plasma formation in the cusp

- Measurements on plasma density, magnetic flux and electron temperature

3. High energy electron injection to high β cusp

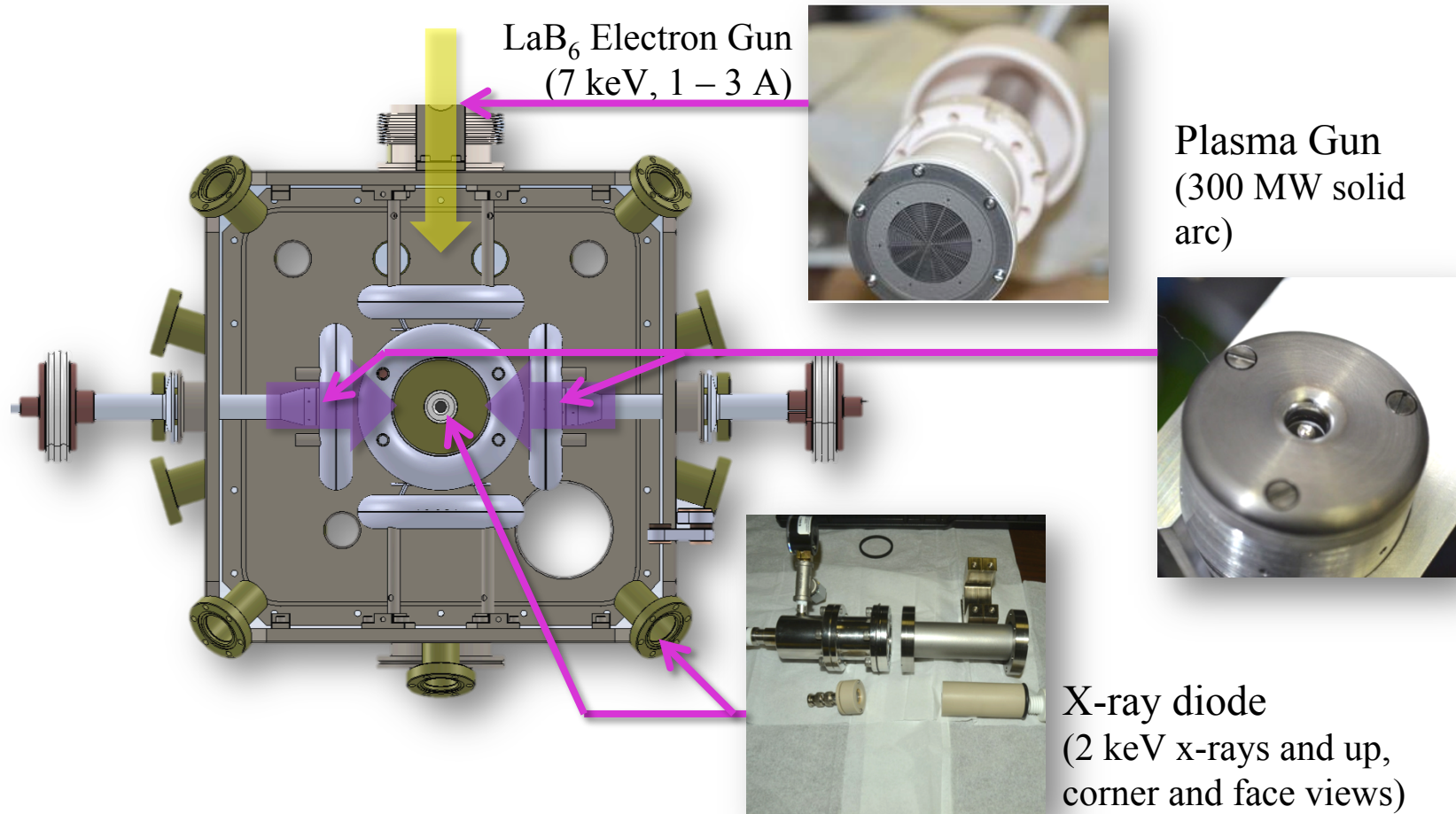
- LaB₆ based electron beam injector, sufficient for diagnostics but not for potential well formation

4. Confinement measurement of high energy electrons in the cusp

- Time resolved hard x-ray intensity from bremsstrahlung

Bulk (cold & dense) plasma from arc injectors provides plasma pressure (high β) to modify cusp B-fields, while the confinement property is measured for high energy electrons in the cusp.

Experimental Setup for high β cusp confinement

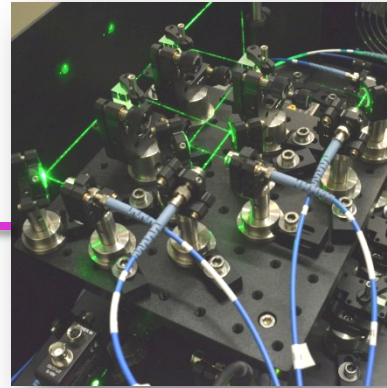


Chamber size: 45 cm cube, Coil major radius; 6.9 cm

Distance between two coils: 21.6 cm, B-field at cusp (near coil center) 0.6 – 2.7 kG

Experimental Setup (continued)

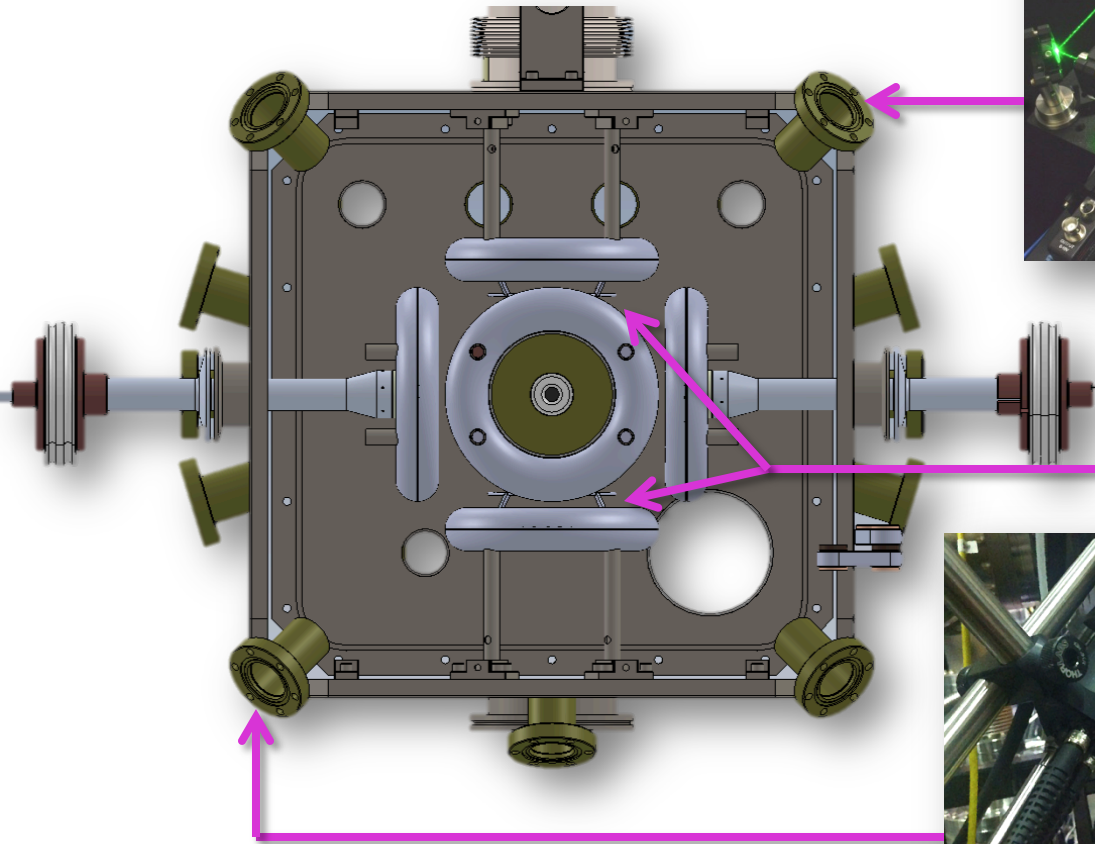
Laser Interferometer
(532 nm, 10^{15} - 10^{17} per cc)



Magnetic Flux
Loops



Photodiodes and
Spectrometer
(Filtered for H_{α} and C_{I-II} ,
High resolution spectrometer,
fiber coupled)



Solid arc plasma injector

Plasma injection by co-axial guns ($j \times B$) using solid fuel

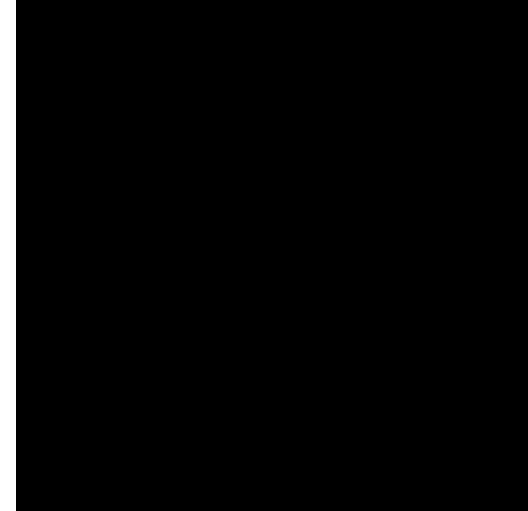
- Ignitron based pulse power system (40 μF cap holds 3 kJ at 12kV)
- ~ 100 kA arc current \rightarrow ~ 300 MW peak power and ~ 7 μs pulse
- $\beta=1$ @ 2.5 kG: 1.5×10^{16} cm^{-3} at 10 eV or 100J in a 10 cm radius sphere



solid arc using
polypropylene film
2 mm A-K gap

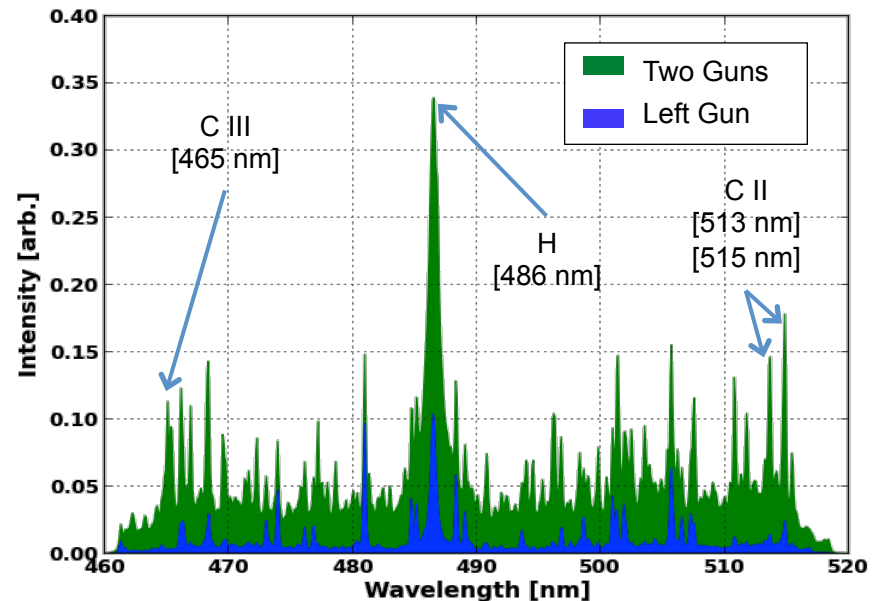
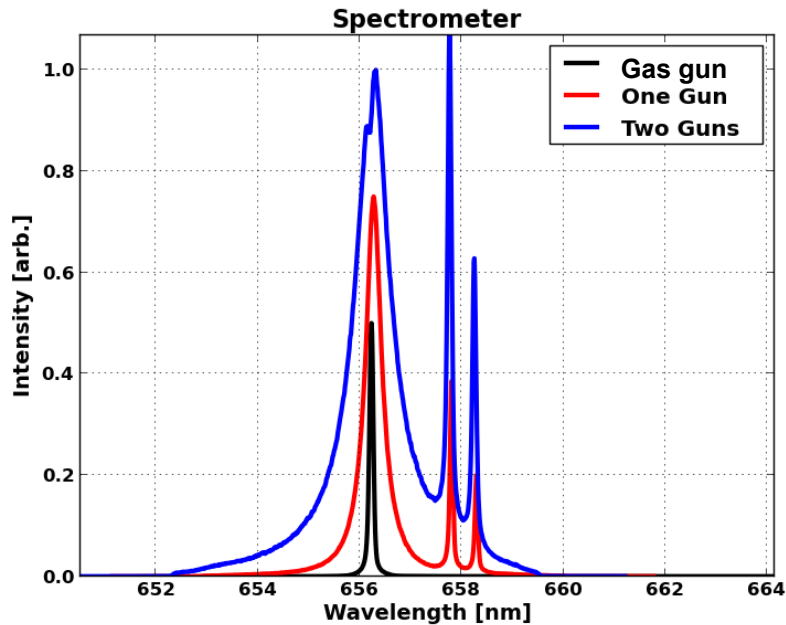


Animation of plasma injection



Dual arc plasma injection movie

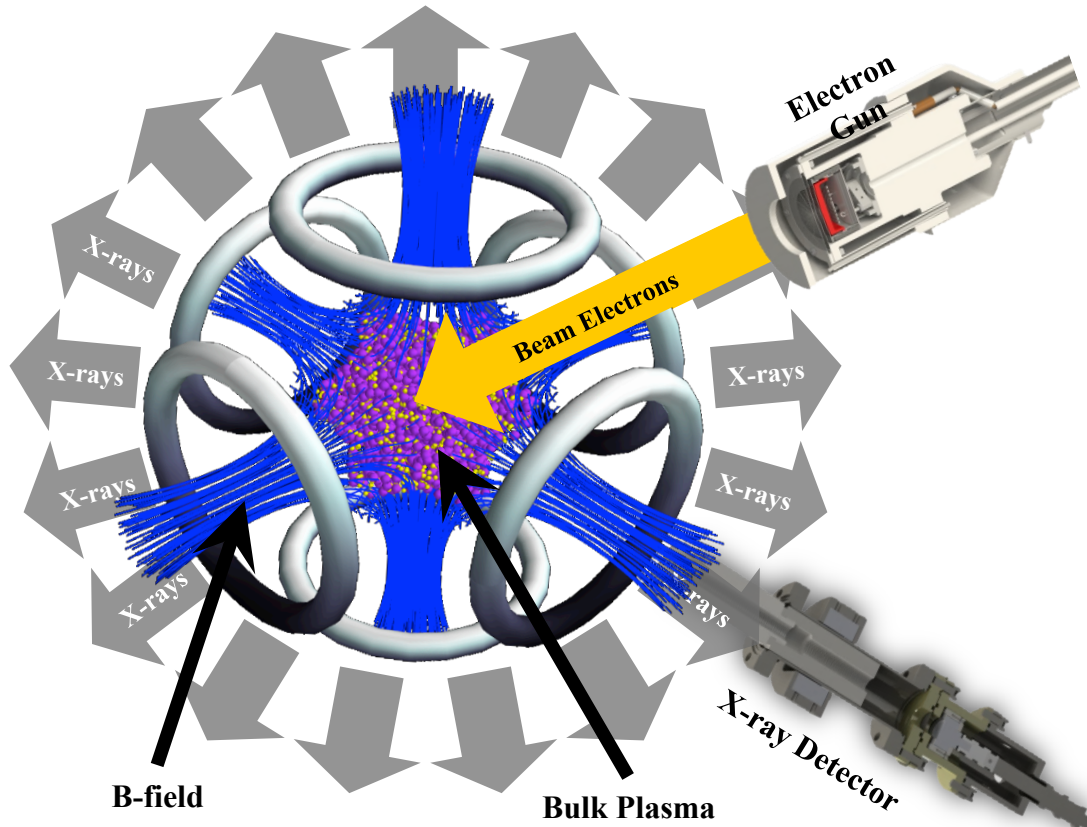
High β plasma formation



- Plasma density on the order of 10^{16} cm^{-3} from Stark broadening of $\text{H}\alpha$ line
- Laser interferometer provides single shot line integrated density variation in time

- Electron temperature is estimated $\sim 10 \text{ eV}$ from C II and CIII emission
- $\text{H}\alpha$, C II line by photodiode and visible spectra by gated CCD is used to monitor T_e variation in time

High energy electron beam produces hard x-rays



E-gun injects
Beam Electrons (7 keV)

Beam electron confinement by
Cusp magnetic fields

Collisions with bulk plasma
create hard x-rays ($E > 2$ keV)
via Bremsstrahlung

Transit time: ~ 7 ns for 7 keV electron for 22 cm transit

Expected confinement time: ~ 45 ns for low β and ~ 18 μ s for high β (x400 increase)

Bremsstrahlung x-ray emission

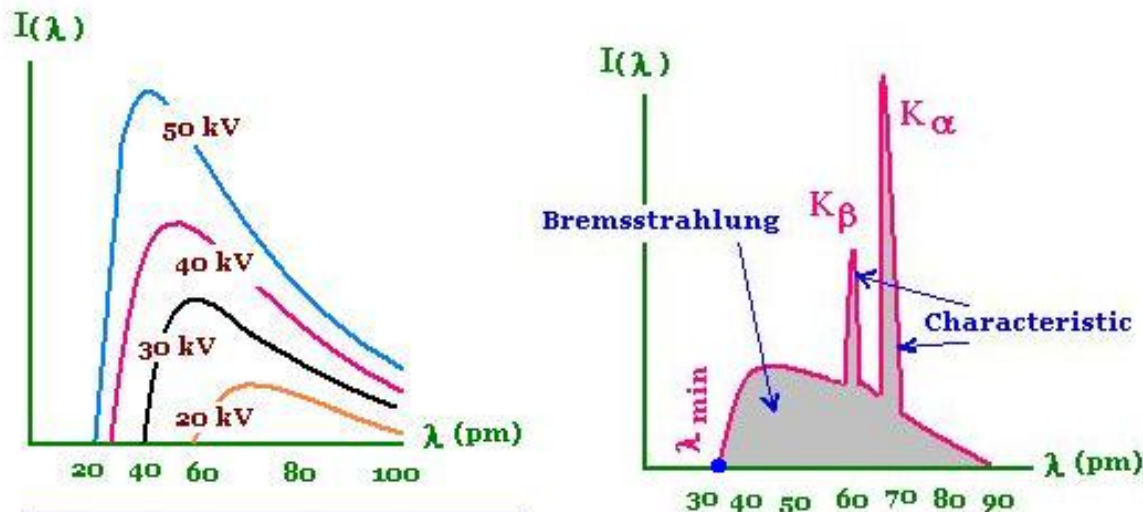
from interaction between beam electrons and plasma

Bremsstrahlung radiation from e-beam interaction with plasma ions

$$e + \text{ion} \rightarrow e + \text{ion} + h\nu \quad \longrightarrow \quad P^{Br} \propto n_e^{beam} E_{beam}^{1/2} n_{ion} Z_{eff}^2$$

Bremsstrahlung x-ray intensity

→ Direct measurement of beam e-density inside Cusp

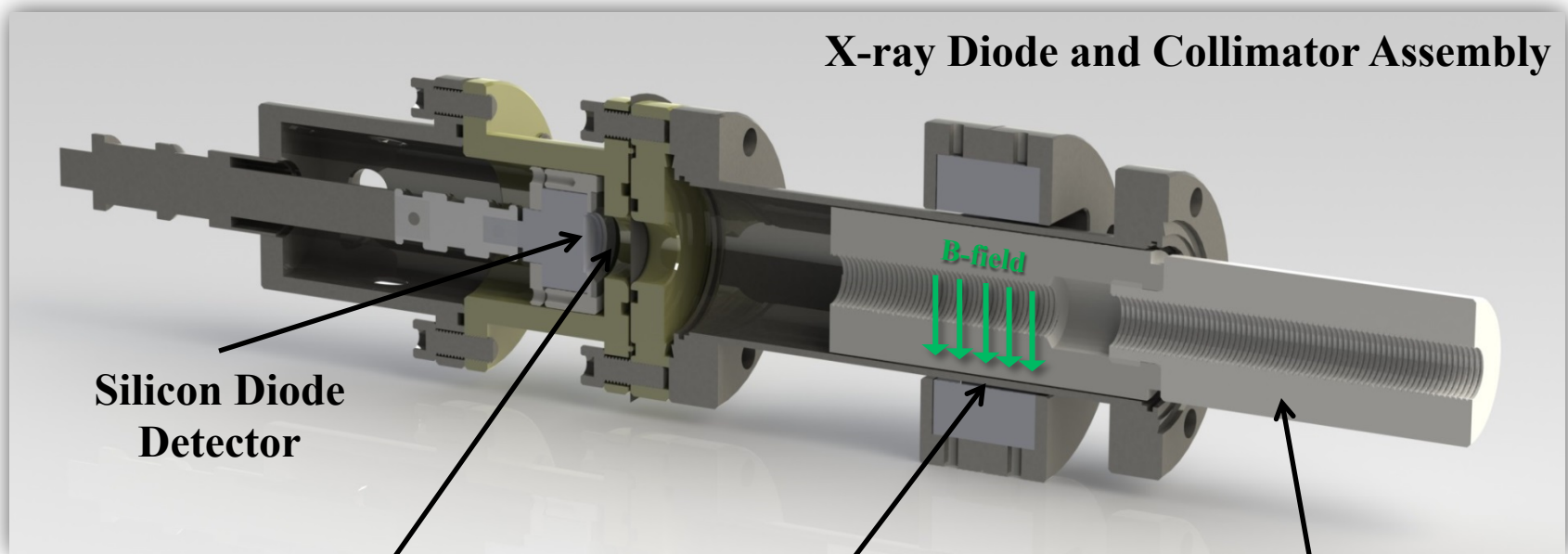


Typical beam target x-ray spectrum

Careful measurement is required to eliminate spurious radiation from impurities, vacuum wall, coil surfaces, and characteristic line emission

X-ray collecting optics to eliminate unwanted signals

X-ray Diode and Collimator Assembly



**Silicon Diode
Detector**

Kapton-Black Film

- Blocks plasma
- Blocks soft x-rays
- Blocks visible light

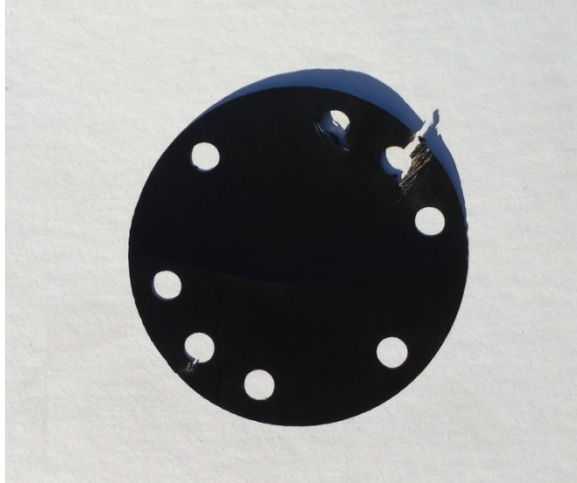
Magnetic Yoke

- Blocks beam electrons

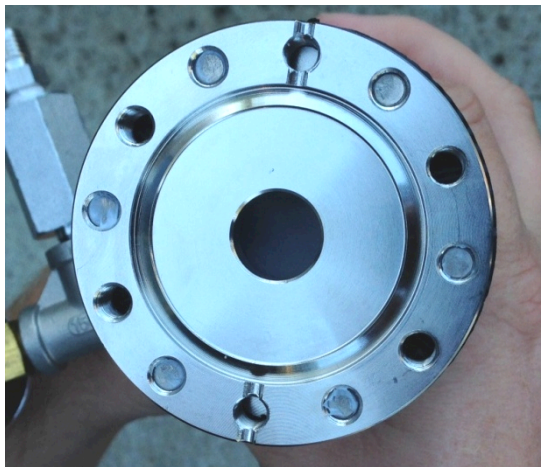
Collimator Tube

- Limits view to plasma
- Plastic material minimizes x-ray production inside tube

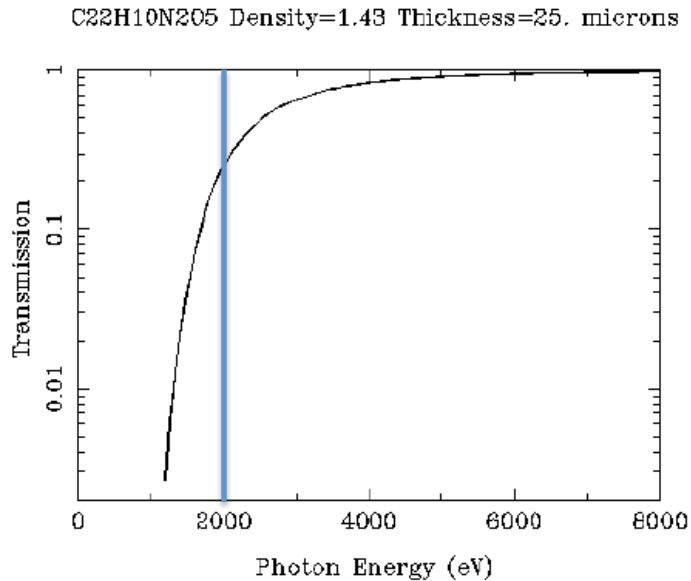
Hard x-ray filter



25 μm thick light tight Kapton filter
(works as vacuum interface)



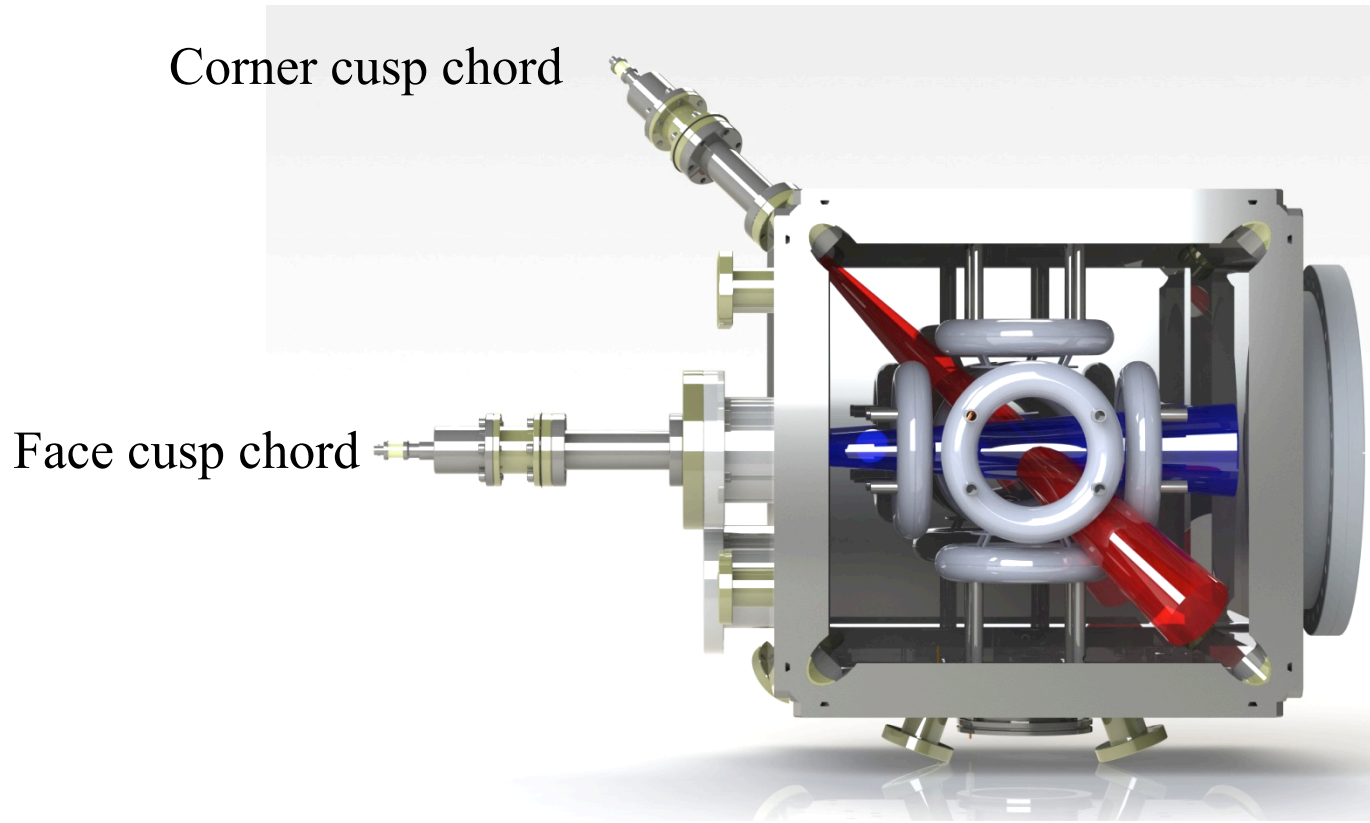
Filter Transmission



Filter has sharp cutoff at ~ 2 keV photon energy

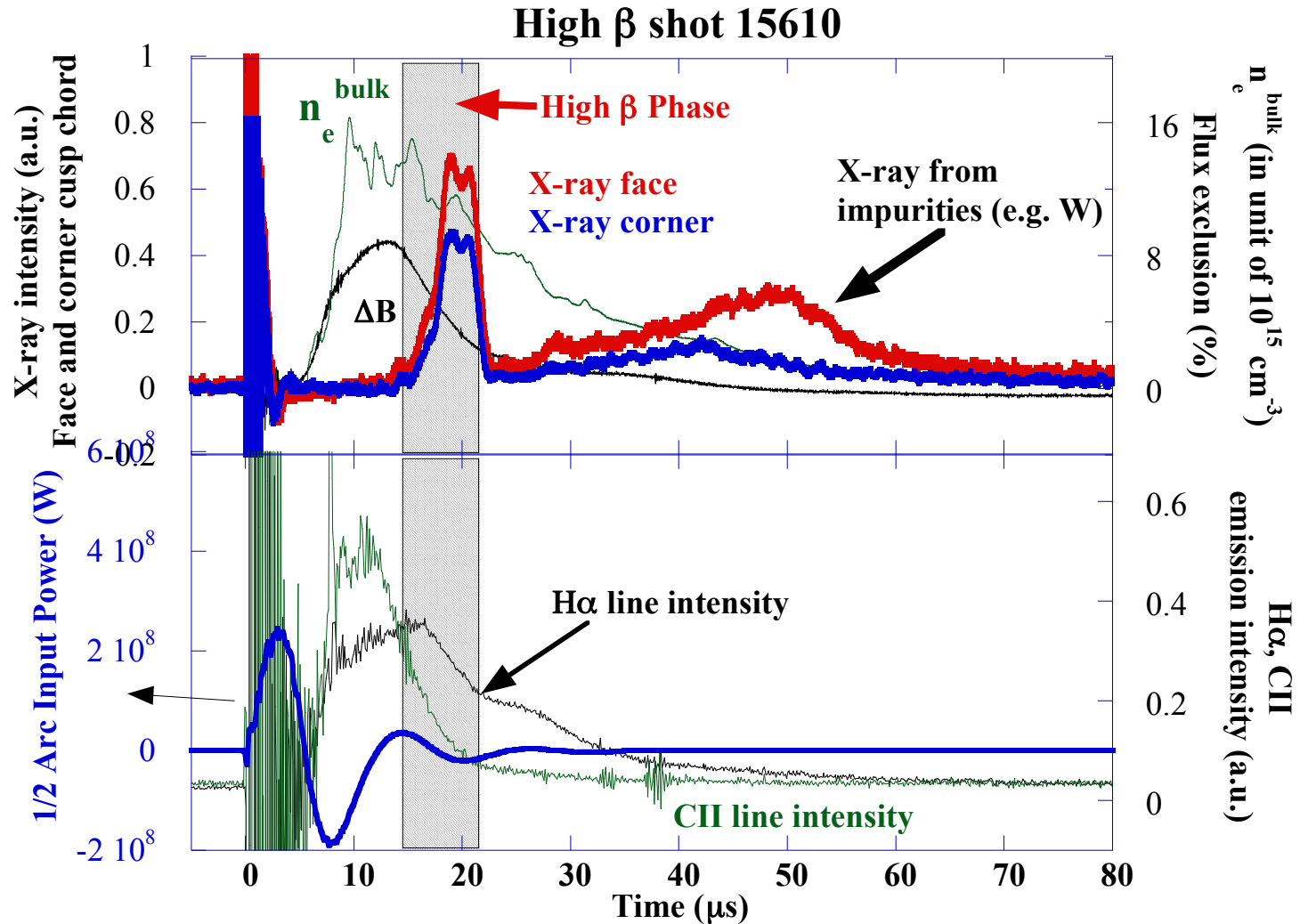
- blocks any characteristic x-ray emission from light elements up to ^{14}Si and ^{15}P
- blocks UV-visible light from plasmas
- blocks charged particles from reaching the detector

Spatial collimation of x-ray detectors



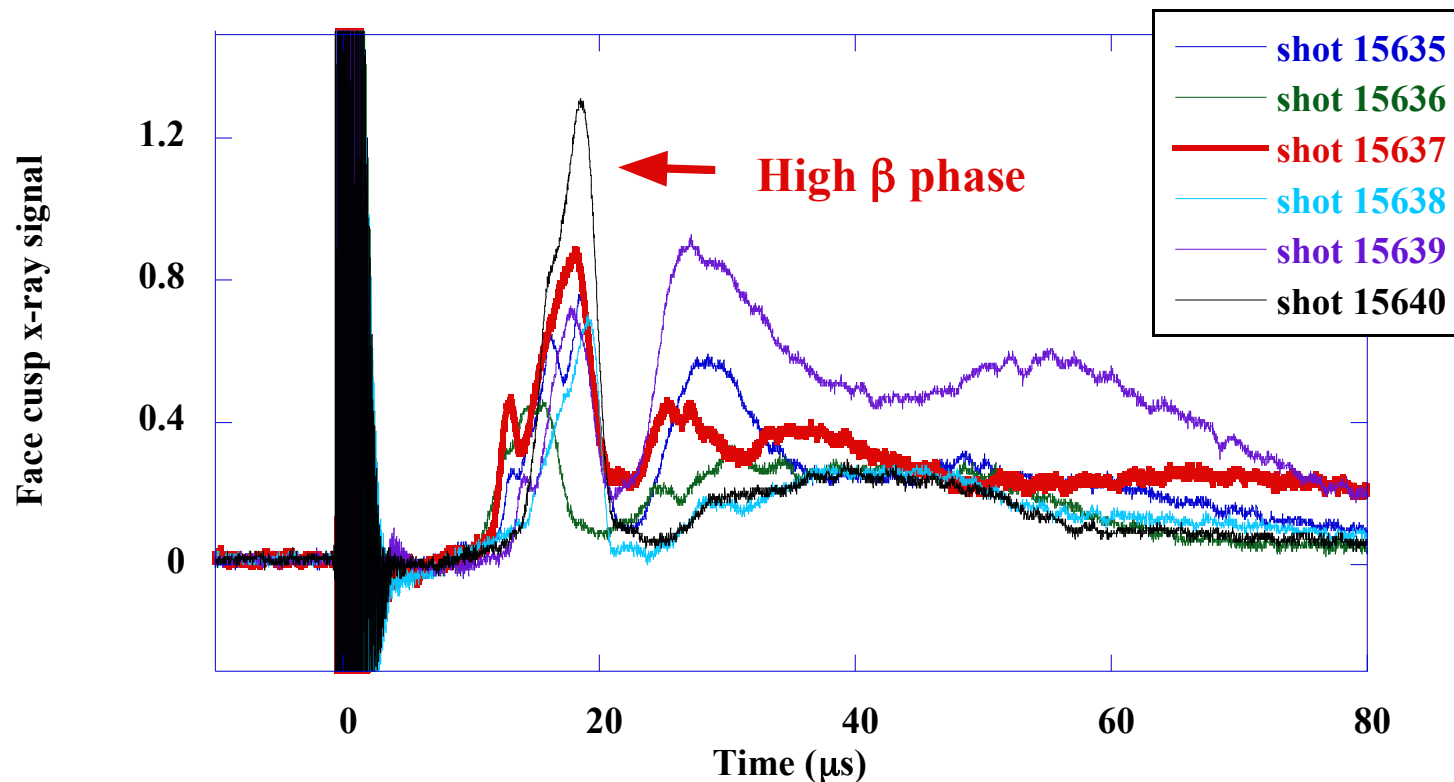
- Collimation is designed to eliminate direct line-of-sight view of metal surfaces
- In addition, opposite sides of the chamber wall are covered using Kapton film and quartz window
- Both chords allow [good volume averaging](#) of x-ray emission from core plasmas

First ever confirmation of high β cusp confinement enhancement (October 23, 2013)



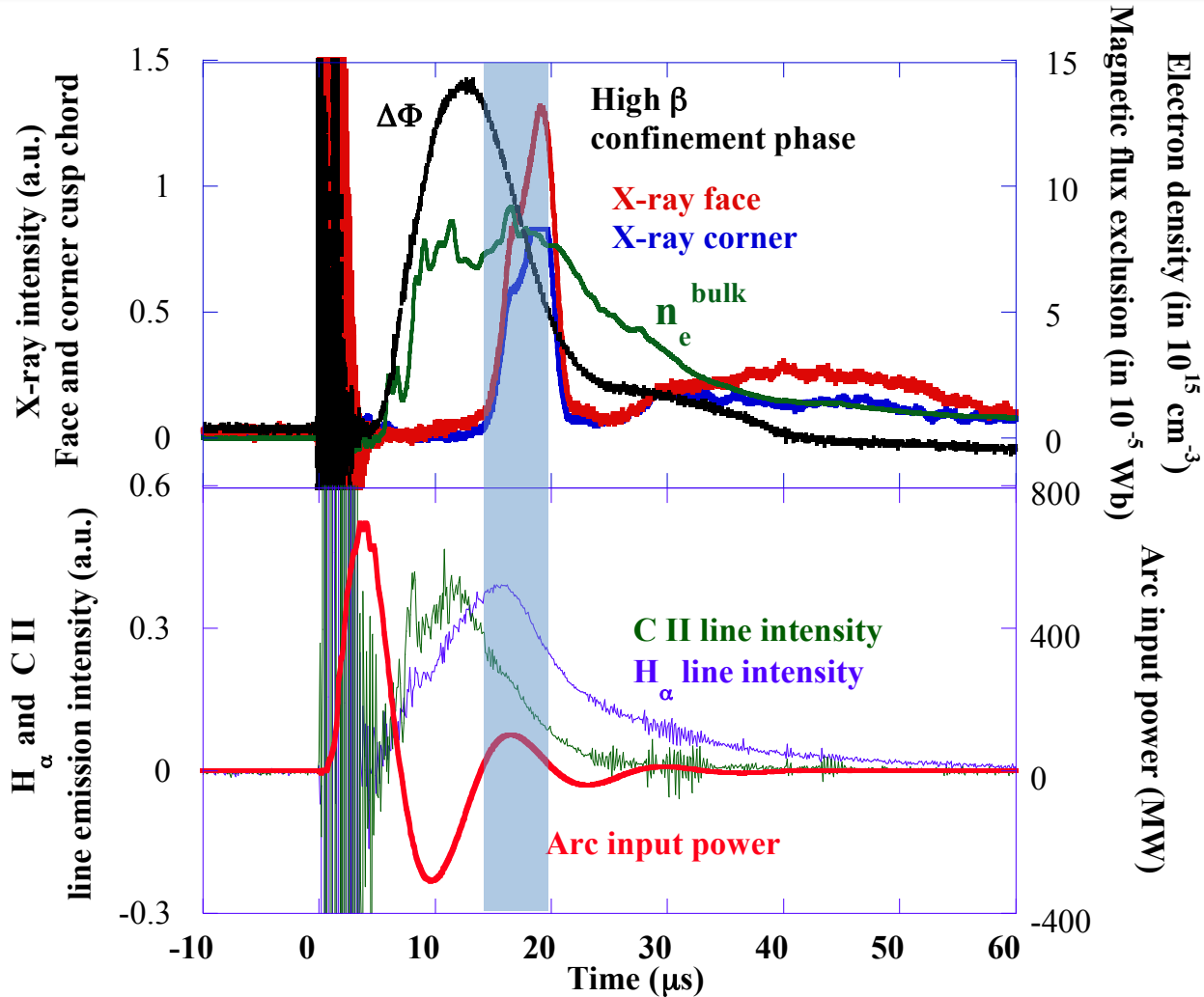
Reproducibility of high β cusp confinement

6 consecutive shots with ~ 200 J of injected plasma energy at 2.7 kG B-fields
→ estimated beta ~ 0.7 and 10% measured flux exclusion



All six shots show distinctive high β phase → good reproducibility

High β cusp shot 15640 (Oct 25, 2013)

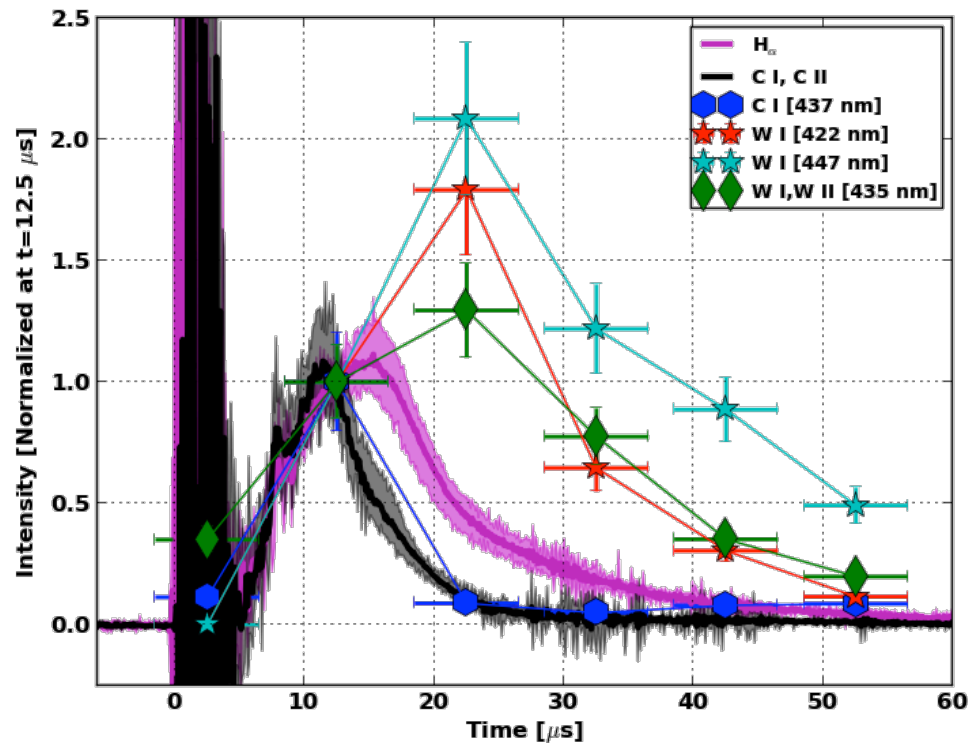


- Hard x-ray signals exhibit very distinctive features between 14 μs and 19 μs

How to interpret x-ray signals

- We have a set of data which shows that the broad x-ray peaks between 40-50 μs come from e-beam interaction with Tungsten impurities.
- Electron beam turns on 30 μs before plasma injection and turns off at $t=150 \mu\text{s}$
- X-ray intensity is low (nearly zero) initially even after bulk density reaches its peak following plasma injection.
- Onset of the x-ray signal increases comes shortly after the peak of flux exclusion
- During the high β phase, the hard x-ray intensity from beam electron interaction with bulk plasma increases by a factor of ~ 20 or more, while the bulk plasma density varies less than a factor of 2.
- At the end of the high β phase, the x-ray signals decrease very rapidly within 1-2 μs . No other plasma quantities change this fast during this period. Since the x-ray measurement is volume averaged, the only possible explanation is a sudden decrease of beam electron confinement.
- Decay of high β phase is expected since arc injectors were designed to inject high β plasma in the cusp but not to sustain it.

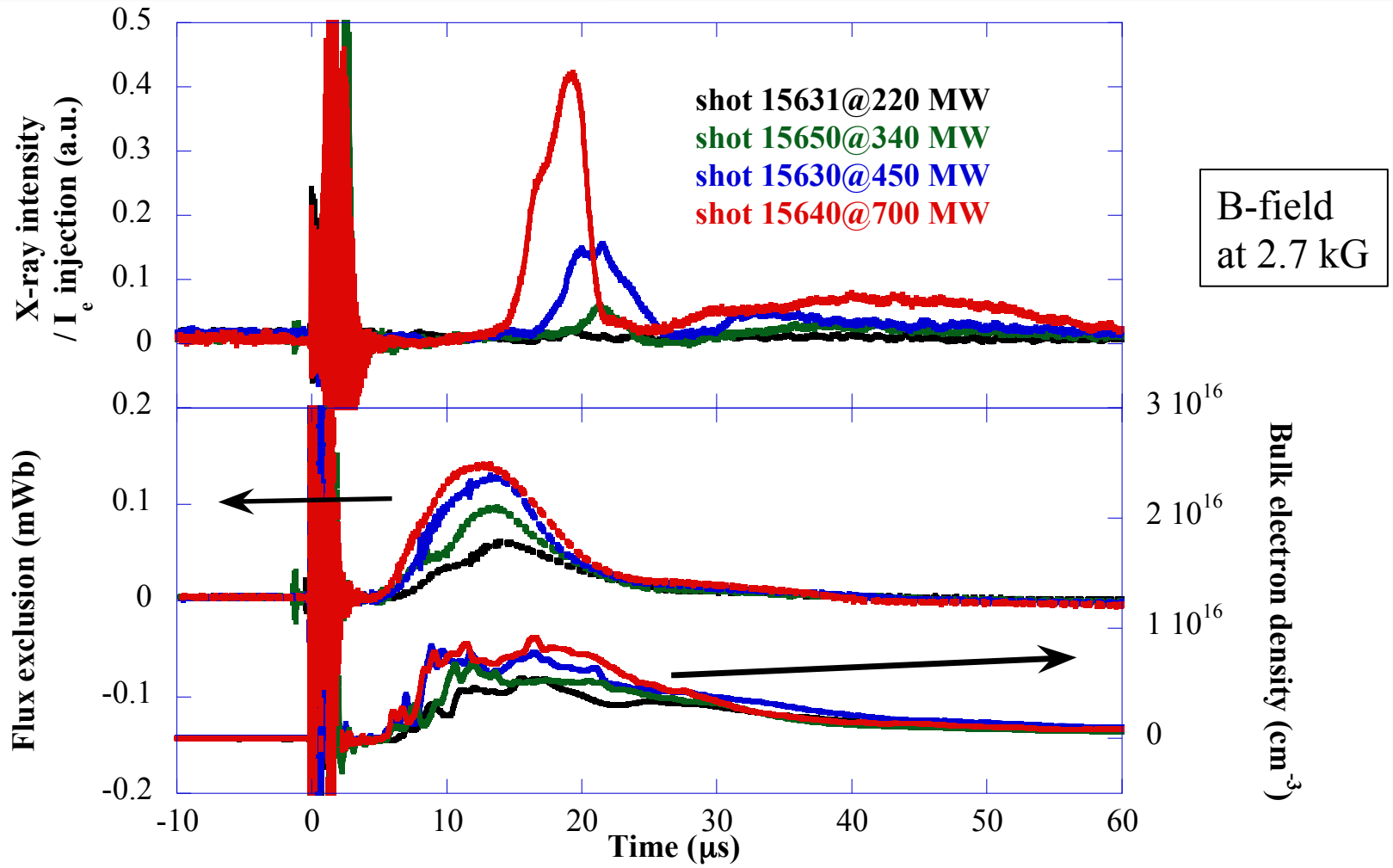
Time resolved spectroscopy on W-impurity



Tungsten cathode
after 200 shots

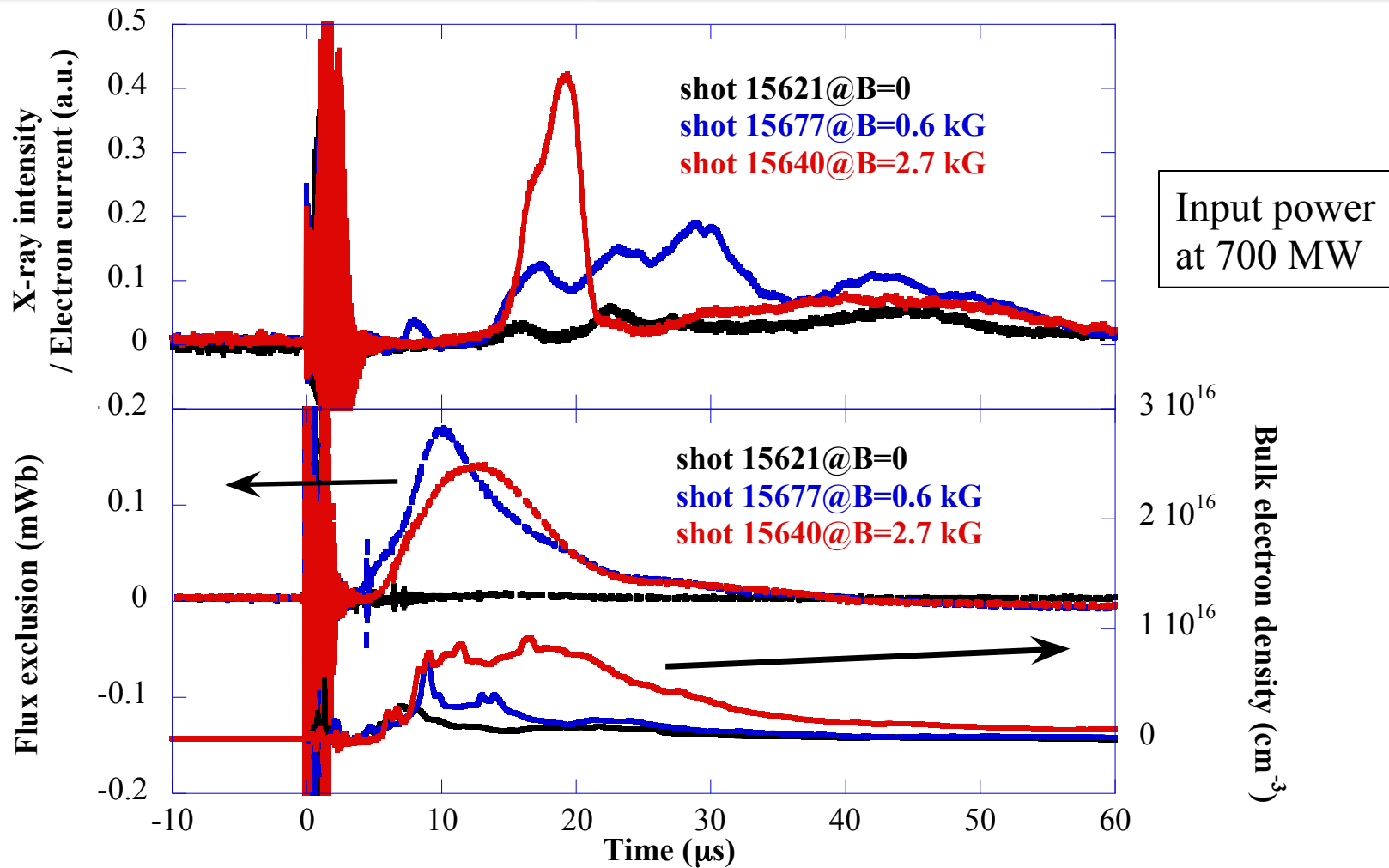
- Line emission intensities from main ion species (H and C) decay early
 - Despite plasma density decay (& cooling of plasma), Tungsten line intensities peak later in time and decay slowly --> indicates gradual build up of Tungsten impurity.
- > **x-ray peak late in the shot (40-50 μs) is from e-bam interaction with Tungsten**

Cusp confinement vs. Injection input power



Cusp confinement enhancement requires sufficiently high β plasma condition

Cusp confinement vs. initial B-fields



No confinement enhancement at B=0 but we need to do more to understand B-field effects

Our Findings on High β Cusp Confinement

Increase in X-ray signal

- Coincides with high β plasma state in the cusp
- Only observed when there is sufficient flux exclusion or plasma injection reaches a threshold
- Peak increase is 10-20x or more compared to low β state
- Exhibits asymmetrical time behavior: gradual increase followed by rapid decrease
- Clearly separated from W impurities injection in time domain

We believe our x-ray measurements unambiguously validate the enhanced electron confinement in a high β cusp compared to a low β cusp

Unresolved issues on high β cusp

1. Decay of good confinement phase

- Decay mechanism: plasma loss/plasma cooling or magnetic field diffusion or something else
- How to extend high β state and prevent the decay

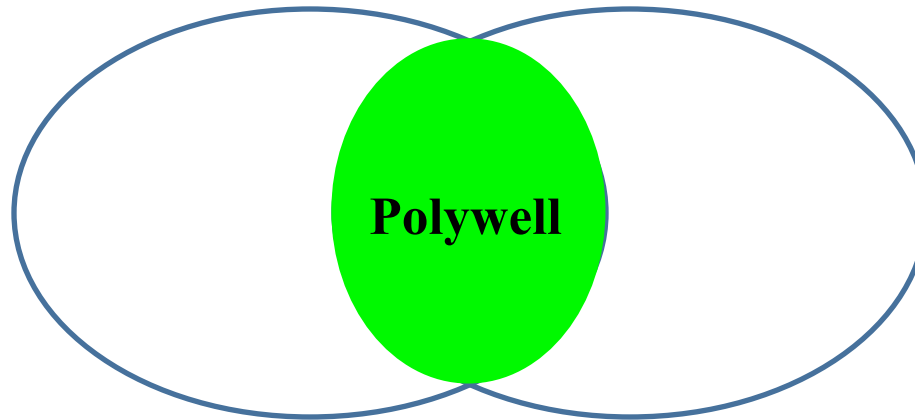
2. Topological information on cusp magnetic fields during high β state

- Thickness of transition layer
- Magnetic field lines near the cusp openings

Future Work

High β cusp
(Confinement of energetic electrons)
Proven in 2013

Electric fusion
(Potential well for energetic ions)
Proven in 1995



High β cusp + Electric fusion at the same time

Summary

- Time resolved hard x-ray measurement provide the first ever direct and definitive confirmation of enhanced plasma confinement in high β cusp, a theoretical conjecture made by Grad and his team in 1950s.
- The enhanced electron confinement in high β cusp allows the Polywell fusion concept to move forward to complete the proof-of-principle test.
- If proven, Polywell device may become an attractive fusion reactor due to the following attributes
 - stable high pressure operation from cusp
 - good electron confinement by high β cusp
 - ion acceleration and confinement by electric fusion

Supplemental Slides

Fusion Research in 1958

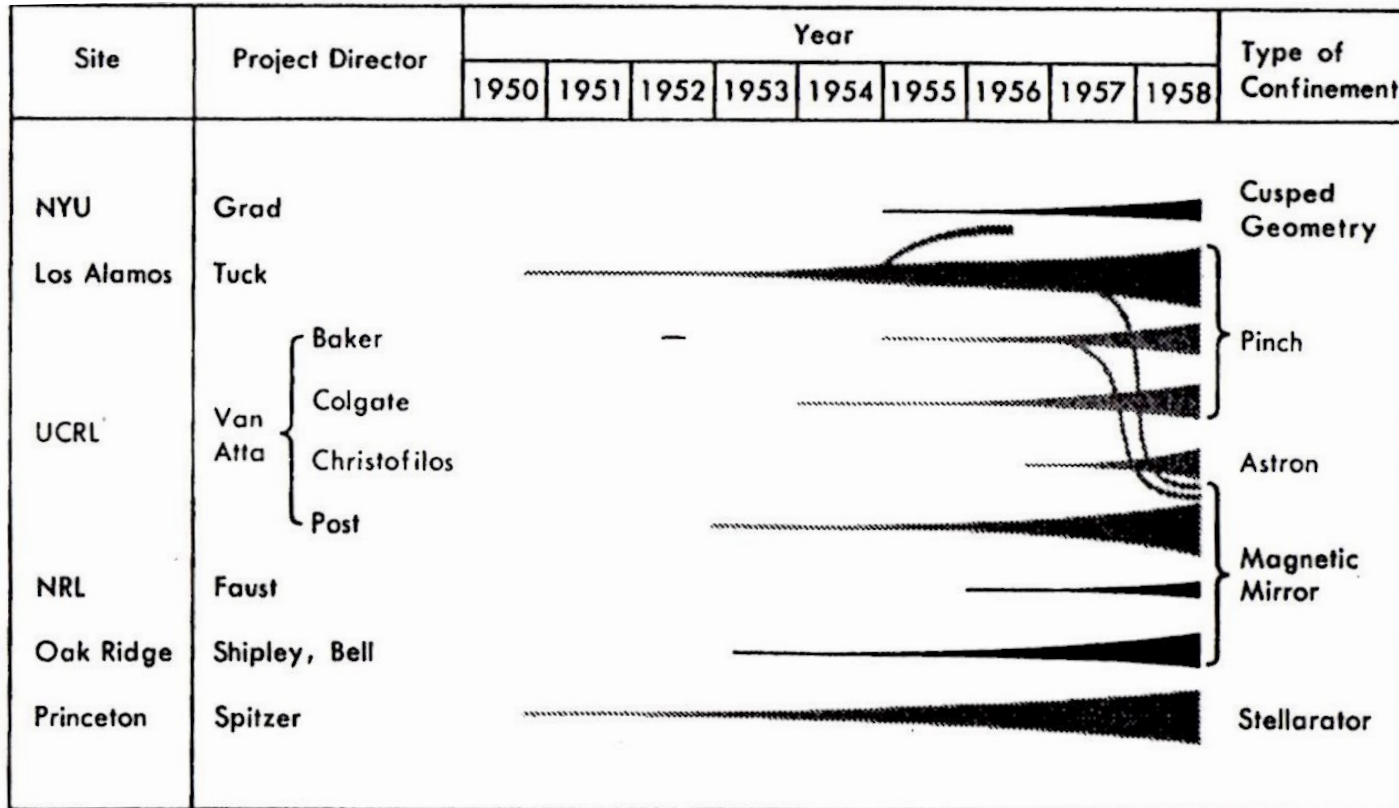
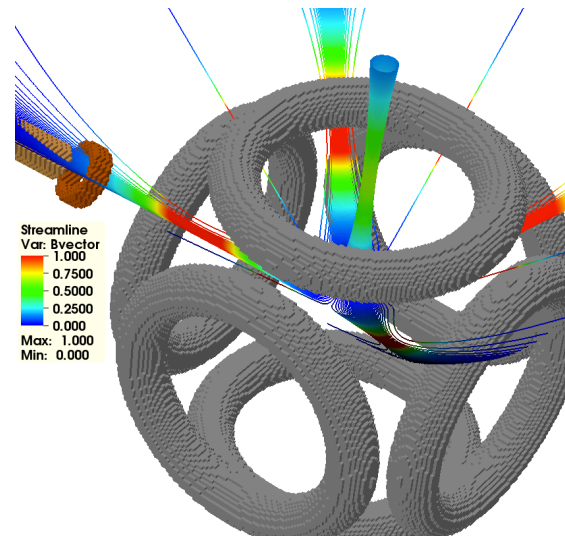
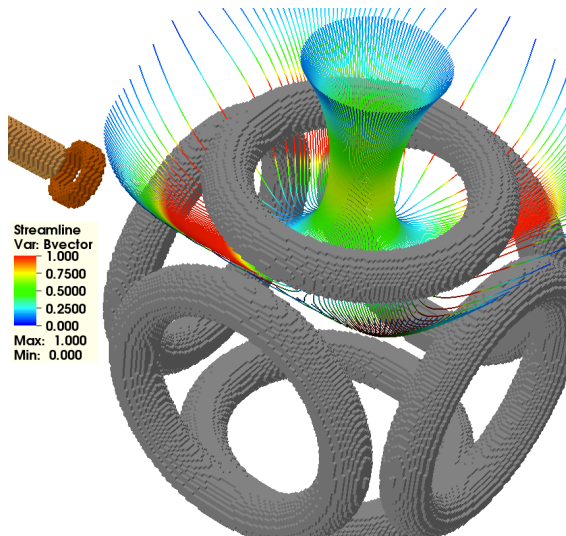
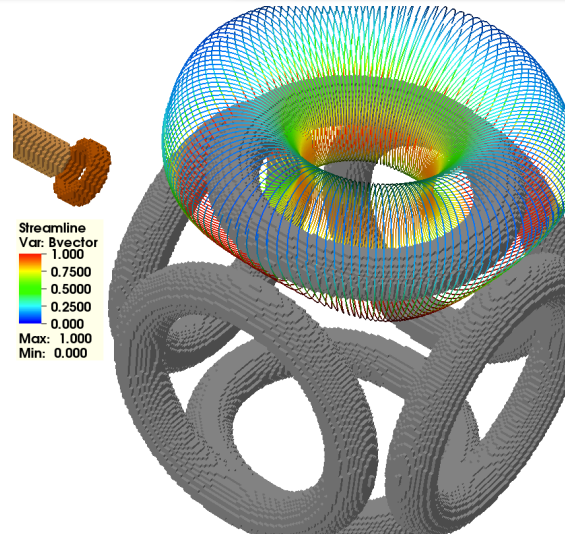
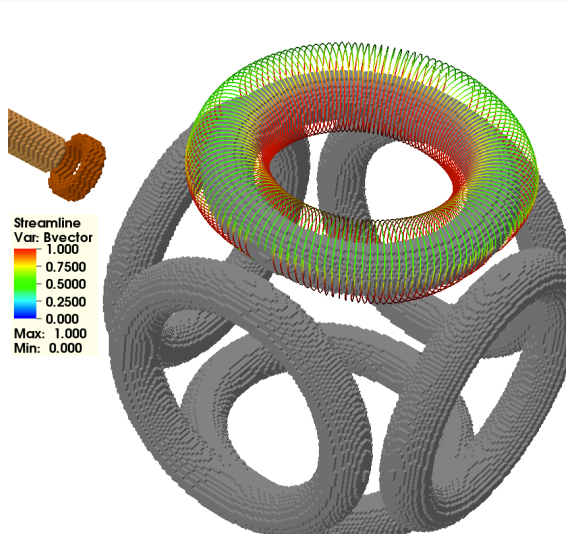


FIG. 19-2. CHRONOLOGY OF THE SHERWOOD PROGRAM, showing methods of plasma confinement in experiments to date.

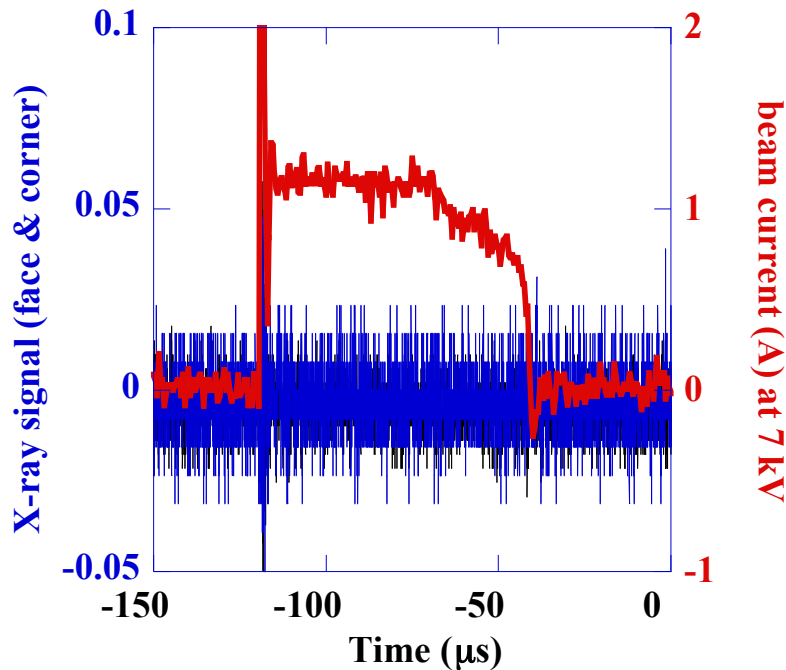
From "Project Sherwood: The U. S. Program in Controlled Fusion" by Amasa Bishop (1958).

Polywell Cusp Magnetic Fields



*6 coil Polywell
magnetic field lines*

Confirmation of X-ray collimation



- e-beam into vacuum magnetic field (no plasma) generates no x-ray response from the diode detector
- Indication of well collimated x-ray optics

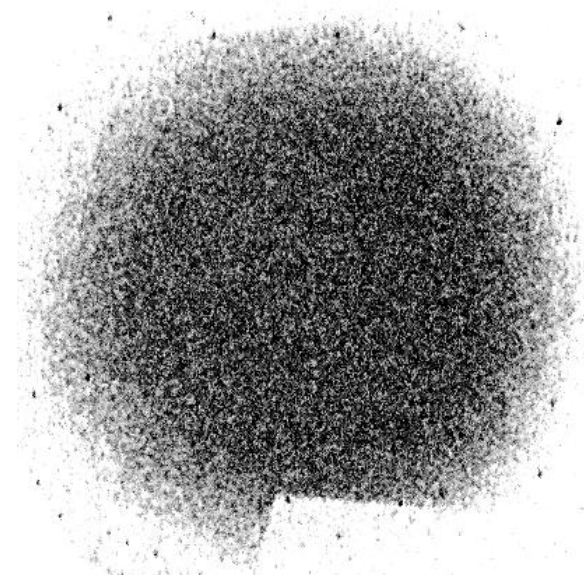
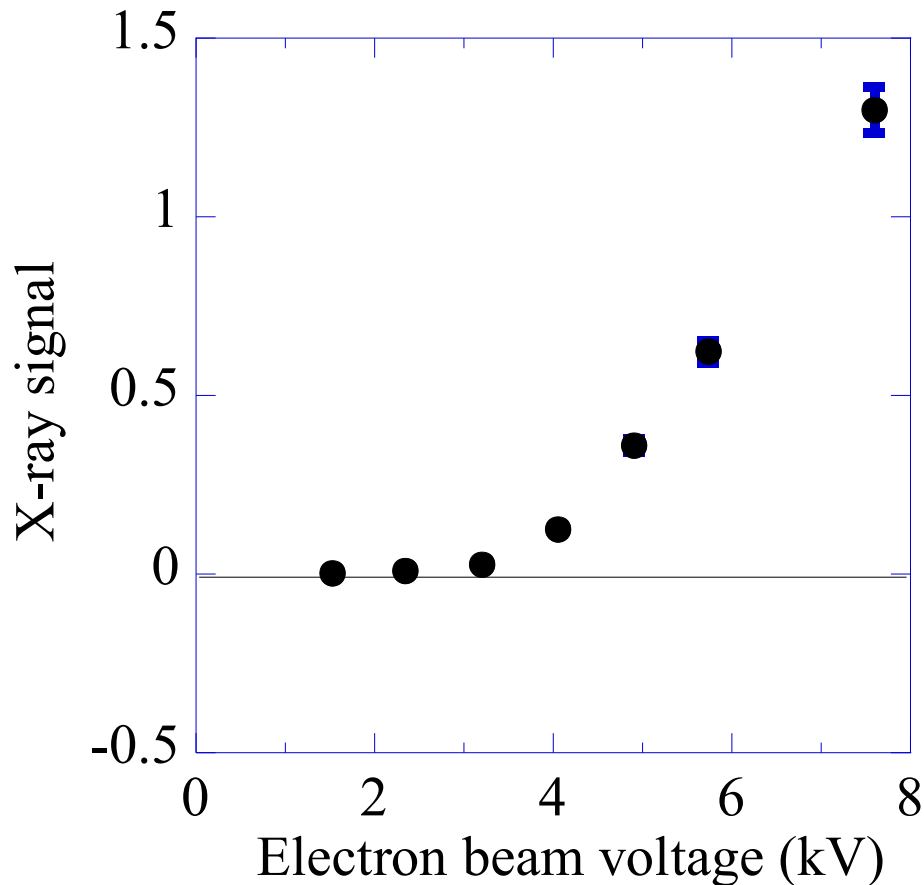


Image plate (x-ray film) exposure at the face cusp detector location

- Uniform exposure
- No sign of spatial structure from coils & walls
- 10 mTorr N₂ gas target
- 20 ms exposure with 4A@7 kV e-beam
- B-field at 1.4 kG

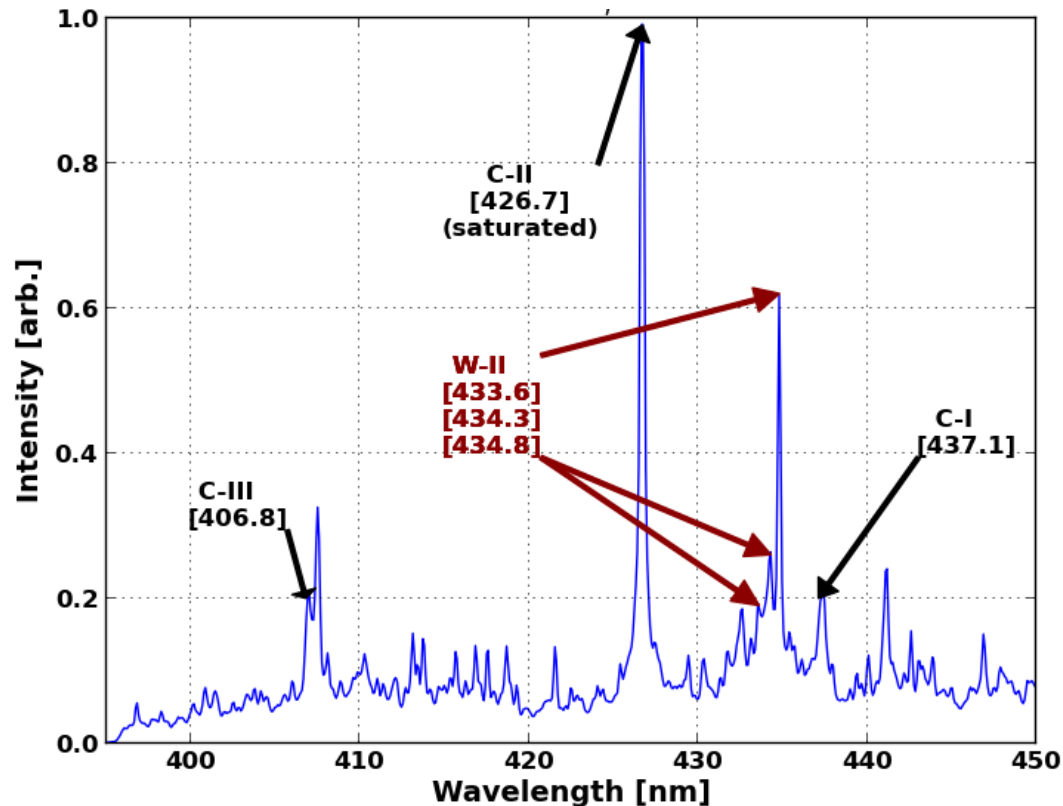
Confirmation of X-ray filter vs. beam energy



- X-ray was generated by electron beam on Stainless Steel target
- 25 μm thick Kapton filter works well to eliminate X-ray photons below 2 keV

Time resolved spectroscopy for impurity transport

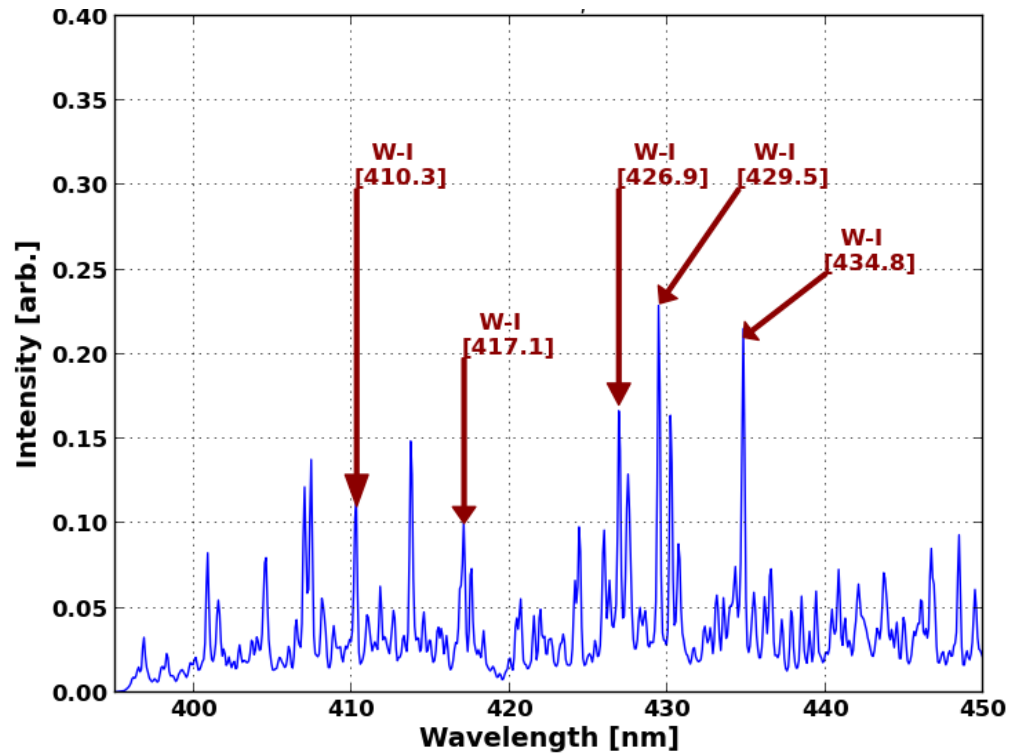
Visible emission spectrum between 12 μs and 20 μs



During the high β phase, plasma emission shows strong C⁺ lines & presence of W⁺ lines
(Note that avg. $n_e \sim 1.5 \times 10^{16} \text{ cm}^{-3}$ and $T_e \sim 10 \text{ eV}$ during this period)

Time resolved spectroscopy (cont.)

Visible emission spectrum between 42 μs and 50 μs

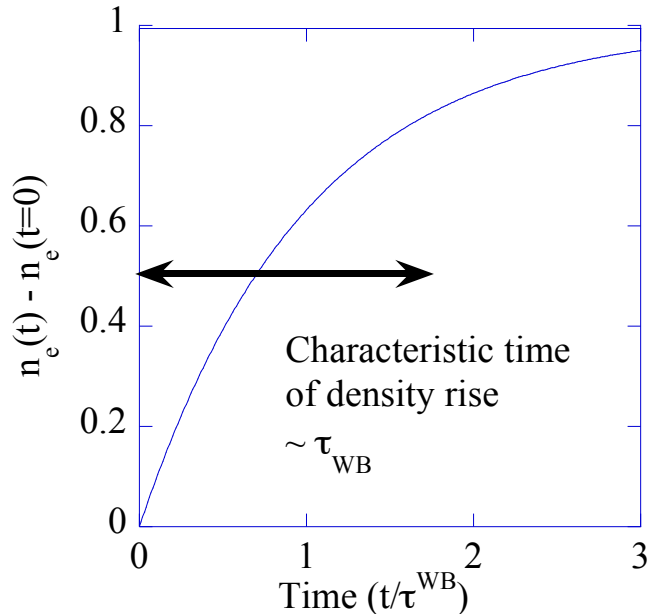


At later time, plasma emission is dominated by W neutral lines, while C^+ and W^+ lines disappear
(Note that avg. $n_e \sim 0.2 \times 10^{16} \text{ cm}^{-3}$ and $T_e < 10 \text{ eV}$)

Estimate of High β Confinement Time

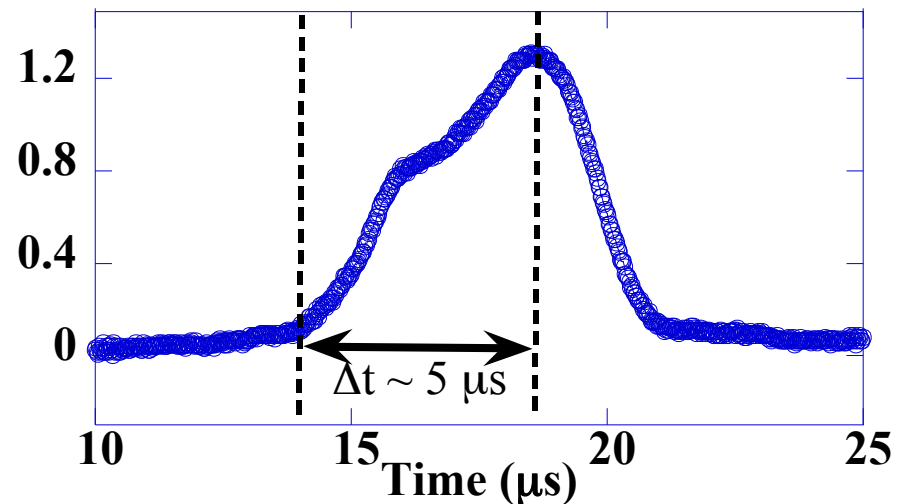
Theoretical model

to estimate high β confinement time



Experimental results

Shot 15640



- Note the shape of x-ray intensity profile: a gradual rise and a rapid drop
- From time response of x-ray signal $\rightarrow \tau > 2.5 \mu s$ ($2 \times \tau \sim$ x-ray signal rise time)
- **$2.5 \mu s$ is about ~ 50 times better than low β cusp confinement time**
- The observed confinement enhancement is very significant and compares well with the theoretically predicted high β cusp confinement time by Grad and his team

Time averaged plasma images



High β cusp formation: intense plasma in the core region